



Investigating genotype-phenotype relationship of extreme neuropathic pain disorders in a national cohort: 'NIHR Bioresources Rare Disease – Neuropathic Pain Disorders'

Journal:	<i>Brain Communications</i>
Manuscript ID	BRAINCOM-2022-323.R1
Manuscript Type:	Original Article
Date Submitted by the Author:	12-Oct-2022
Complete List of Authors:	Themistocleous, Andreas; University of Oxford Nuffield Department of Clinical Neurosciences, Baskozos, Georgios; Oxford University, Nuffield Department of Clinical Neurosciences; Oxford University Blesneac, Iulia; University of Oxford Nuffield Department of Clinical Neurosciences Comini, Maddalena; University of Oxford Nuffield Department of Clinical Neurosciences Megy, Karyn; NIHR BioResource; University of Cambridge, Department of Haematology Chong, Sam ; National Hospital for Neurology and Neurosurgery Deevi, Srivishnuvardhan; NIHR BioResource; University of Cambridge, Department of Haematology Ginsberg, Lionel; Royal Free Campus, University College London, Institute of Neurology Gosal, David; Salford Royal NHS Foundation Trust Hadden, Robert; King's College Hospital NHS Foundation Trust, Neurology Horvath, Rita; Wellcome Centre for Mitochondrial Research; University of Cambridge, Department of Clinical Neurosciences mahdi-Rogers, Mohamed; King's College Hospital NHS Foundation Trust Manzur, Adnan; Great Ormond Street Hospital for Children NHS Foundation Trust; UCL Great Ormond Street Institute of Child Health Population Policy and Practice Mapeto, Rutendo; NIHR BioResource; Cambridge University, Department of Haematology Marshall, Andrew; University of Liverpool, ; The University of Manchester, Matthews, Emma; St George's University Hospitals NHS Foundation Trust, Atkinson Morley Neuromuscular Centre; St George's University of London, McCarthy, Mark; NIHR Oxford Biomedical Research Centre; Wellcome Trust Centre for Human Genetics; University of Oxford, Oxford Centre for Diabetes, Endocrinology and Metabolism Reilly, Mary; UCL, Institute of Neurology Renton, Tara; King's College Hospital NHS Foundation Trust Rice, Andrew; Imperial College London, Pain Research, Department of Surgery and Cancer

1
2
3
4
5
6
7
8
9
10
11
12
13
14
15
16
17
18
19
20
21
22
23
24
25
26
27
28
29
30
31
32
33
34
35
36
37
38
39
40
41
42
43
44
45
46
47
48
49
50
51
52
53
54
55
56
57
58
59
60

	Vale, Tom; University of Oxford Nuffield Department of Clinical Neurosciences van Zuydam, Natalie; NIHR Oxford Biomedical Research Centre; Wellcome Trust Centre for Human Genetics; University of Oxford, Oxford Centre for Diabetes, Endocrinology and Metabolism Walker, Suellen; UCL GOS Institute of Child Health, Clinical Neurosciences (Pain Research); Great Ormond Street Hospital For Children NHS Foundation Trust, Dept of Anaesthesia and Pain Medicine Woods, Geoff; Addenbrookes Hospital, Cambridge Institute of Medical Research Bennett, David; University of Oxford Nuffield Department of Clinical Neurosciences,
Keywords:	Neuropathic pain, Whole genome sequencing, Peripheral neuropathy, Sodium channels

SCHOLARONE™
Manuscripts

Investigating genotype-phenotype relationship of extreme neuropathic pain disorders in a national cohort: 'NIHR Bioresources Rare Disease – Neuropathic Pain Disorders'

Andreas C. Themistocleous^{1*}, Georgios Baskozos^{1*}, Iulia Blesneac^{1,*}, Maddalena Comini^{1*}, Karyn Megy^{2,3,*}, Sam Chong⁴, Sri VV Deevi^{2,3}, Lionel Ginsberg^{5,6}, David Gosal⁷, Robert DM Hadden⁸, Rita Horvath^{9,10}, Mohamed Mahdi-Rogers⁸, Adnan Manzur^{11,12}, Rutendo Mapeta^{2,3}, Andrew Marshall^{13,14,15}, Emma Matthews¹⁶, Mark I. McCarthy^{17,18,19}, NIHR BioResource for the 100,000 Genomes Project[¶], Mary M Reilly¹⁶, Tara Renton⁸, Andrew S.C. Rice^{20,21}, Tom A. Vale¹, Natalie van Zuydam^{17,18,19}, Suellen M. Walker^{11,12}, Christopher Geoffrey Woods^{22,23}, David L.H. Bennett¹

¹Nuffield Department of Clinical Neurosciences, University of Oxford, Oxford, UK

²NIHR BioResource, Cambridge University Hospitals NHS Foundation, Cambridge Biomedical Campus, Cambridge, UK;

³Department of Haematology, University of Cambridge, Cambridge Biomedical Campus, Cambridge, UK;

⁴National Hospital for Neurology and Neurosurgery, University College London Hospitals, London, UK

⁵ Department of Neurology, Royal Free Hospital, London, UK

⁶Department of Clinical and Movement Neurosciences, UCL Queen Square Institute of Neurology, Royal Free Campus, London, UK.

⁷Salford Royal NHS Foundation Trust, Salford, UK.

⁸King's College Hospital NHS foundation trust, London, UK

⁹Wellcome Centre for Mitochondrial Research, Institute of Genetic Medicine, Newcastle University, Newcastle upon Tyne, UK

¹⁰Department of Clinical Neurosciences, University of Cambridge, Cambridge, UK

¹¹Great Ormond Street Hospital for Children NHS Foundation Trust, London, UK.

¹²UCL Great Ormond Street Institute of Child Health, London, UK

¹³Faculty of Biology, Medicine and Health, School of Biological Sciences, Division of Neuroscience and Experimental Psychology, University of Manchester, Manchester, UK.

¹⁴Department of Clinical Neurophysiology, Manchester University NHS Foundation Trust, Manchester, Manchester Academic Health Science Centre, Manchester, UK.

¹⁵Institute of Life Course and Medical Sciences, University of Liverpool, Liverpool, UK

¹⁶Department of Neuromuscular Disease, UCL Queen Square Institute of Neurology and the National Hospital of Neurology and Neurosurgery, London, UK

¹⁷NIHR Oxford Biomedical Research Centre, Oxford University Hospitals Trust, Oxford, UK.

¹⁸Wellcome Centre for Human Genetics, University of Oxford, Oxford, UK

¹⁹Oxford Centre for Diabetes, Endocrinology and Metabolism, University of Oxford, Churchill Hospital, Oxford

²⁰Pain Research, Department of Surgery and Cancer, Faculty of Medicine, Imperial College London, London, UK.

²¹Pain Medicine, Chelsea and Westminster Hospital NHS Foundation Trust, London, UK.

1
2
3 ²²Department of Medical Genetics, Cambridge Institute for Medical Research, University of
4 Cambridge, Cambridge Biomedical Campus, Cambridge, UK.

5
6 ²³Addenbrookes Hospital, Cambridge University Hospitals NHS Foundation Trust,
7 Cambridge, UK.
8

9
10 * These authors contributed equally to the work

11 ¶A list of authors and their affiliations appears in the online version of the paper
12
13

14 Corresponding authors:

15 David L.H. Bennett

16 Nuffield Department of Clinical Neurosciences, University of Oxford, Level 6 West Wing,
17 John Radcliffe Hospital, Oxford, OX3 9DU, UK

18 Tel: +44 1865 231512; e-mail: david.bennett@ndcn.ox.ac.uk
19
20

21 Dr Andreas Themistocleous

22 Nuffield Department of Clinical Neurosciences, University of Oxford, Level 6 West Wing,
23 John Radcliffe Hospital, Oxford, OX3 9DU, UK

24 Tel: +44 1865 234839 ; e-mail: andreas.themistocleous@ndcn.ox.ac.uk
25
26

27
28 Current address for Mark McCarthy

29 Genentech, 1 DNA Way, South San Francisco, CA 94080.
30
31

32 Current address for Emma Matthews

33 Atkinson-Morley Neuromuscular Centre, St George's University Hospitals NHS Foundation
34 Trust, and St George's University of London, London, UK
35
36
37
38
39
40
41
42
43
44
45
46
47
48
49
50
51
52
53
54
55
56
57
58
59
60

Abstract

Objective: ~~By integrating whole genome sequencing into healthcare~~ The aims of our study were to use whole genome sequencing in a cross-sectional cohort of patients ~~we aimed to~~ identify new variants in genes implicated in neuropathic pain, to determine prevalence of known pathogenic variants, and understand the relationship between pathogenic variants and clinical presentation.

Methods: Patients with extreme neuropathic pain phenotypes (both sensory loss and gain) were recruited from secondary care clinics in the UK, and underwent whole genome sequencing as part of NIHR-Bioresource. A multi-disciplinary team assessed pathogenicity of rare variants in genes previously known to cause neuropathic pain disorders and exploratory analysis of research candidate genes was completed. Association testing for genes carrying rare variants was completed using the gene-wise approach of the combined burden and variance-component test SKAT-O. ~~Electrophysiological analysis~~ Patch clamp analysis was performed on transfected HEK293T cells ~~was completed~~ for research candidate variants of genes encoding ion channels.

Results:

1) Medically actionable variants were found in 12% of study participants (205 recruited), including known pathogenic variants: *SCN9A*(*ENST00000409672.1*): c.2544T>C, p.Ile848Thr p.I848T that causes inherited erythromelalgia, and *SPTLC1*(*ENST00000262554.2*):c.340T>G, p.Cys133Tr p.C133W variant that causes hereditary sensory neuropathy type-1.

2) Clinically relevant variants were most common in voltage-gated sodium channels.

3) *SCN9A*(*ENST00000409672.1*):c.554G>A, p.Arg185His p.R185H variant was more common in non-freezing cold injury participants than controls, and causes a gain of function of Na_v1.7 after cooling (the environmental trigger for non-freezing cold injury).

4) Rare variant association testing showed a significant difference in distribution for genes *NGF*, *KIF1A*, *SCN8A*, *TRPM8*, *KIF1A*, *TRPA1* and the regulatory regions of genes *SCN11A*, *FLVCRI*, *KIF1A*, and *SCN9A* between European participants with neuropathic pain and controls.

5) The *TRPA1*(*ENST00000262209.4*):c.515C>T, p.A172V p.Ala172Val variant identified in participants with episodic somatic pain disorder demonstrated gain of channel function to agonist stimulation.

Conclusion: Whole genome sequencing identified clinically relevant variants in over 10% of participants with extreme neuropathic pain phenotypes. The majority of these variants were found in ion channels. Combining genetic analysis with functional validation can lead to better understanding as to how rare variants in ion channels lead to sensory neuron hyper-excitability, and how cold, as an environmental trigger, interacts with the gain of function Na_v1.7 p.Arg185His R185H variant. Our findings highlight the role of ion channel variants in the pathogenesis of extreme neuropathic pain disorders, likely mediated through changes in sensory neuron excitability and interaction with environmental triggers.

Introduction

Neuropathic pain occurs as a consequence of a disease or lesion in the somatosensory nervous system (Treede *et al.*, 2008). It affects 6.9-10% of the general population (van Hecke *et al.*, 2014) and has a harmful impact on physical health, psychological health and quality of life (Attal *et al.*, 2011). Understanding the role of genetic factors in neuropathic pain may reveal new pathophysiological mechanisms and is under-explored (Hébert *et al.*, 2017; Calvo *et al.*, 2019).

Extreme pain phenotypes, caused by rare high-impact genetic mutations, offer insight into fundamental neurobiological mechanisms of pain (Bennett and Woods, 2014). The phenotypes can range from congenital insensitivity to pain (Schon *et al.*, 1993) to enhanced pain perception. Different types of mutations in the same gene can cause a spectrum of phenotypes. For example, biallelic loss of function mutations in *SCN9A*, the gene encoding the voltage-gated sodium channel (Na_v) 1.7 and which is highly expressed in peripheral sensory neurons (Bennett *et al.*, 2019), causes congenital insensitivity to pain (Cox *et al.*, 2006). In contrast, monoallelic gain of function variants in the same gene are associated with pain disorders, which are inherited in a Mendelian fashion. These include inherited erythromelalgia (Yang *et al.*, 2004) and paroxysmal extreme pain disorder (Fertleman *et al.*, 2006).

Variants in genes causing Mendelian pain disorders may act as risk factors for common acquired neuropathic pain disorders. For example, *SCN9A* variants are implicated in more common neuropathic pain disorders such as idiopathic small fibre neuropathy (Faber *et al.*, 2012a) and painful diabetic neuropathy (Blesneac *et al.*, 2018). The *SCN9A* NM_002977.3:c.3448C>T, [p.R1150Wp.Arg1150Trp](#) variant modulates risk and severity of pain across different chronic pain disorders (Reimann *et al.*, 2010). An environmental trigger that interacts with genes may cause neuropathic pain as some variants are common in the general population. Identification of such gene variants is important in diagnosis, genetic counselling and treatment enabling a stratified approach, such as the use of sodium channel blockers (e.g. lacosamide) in patients with small fibre neuropathy and gain-of-function Na_v 1.7 variants (Labau *et al.*, 2020). In some cases, such as inherited erythromelalgia, a personalised management approach can be used (Yang *et al.*, 2012; Geha *et al.*, 2016). Furthermore, there are rare inherited conditions where direct treatment can arrest progression, such as Fabry's disease and hereditary transthyretin amyloidosis. In these diseases neuropathic pain is often the first symptom, the disease will progress if untreated and timely genetic diagnosis is essential to initiate appropriate treatment (Carroll *et al.*, 2022).

The National Institute of Health Research (NIHR) BioResource Rare Disease project applied whole genome sequencing to a range of rare diseases, including Neuropathic Pain Disorders (Turro *et al.*, 2020). The aims of our study were to aid the genetic diagnosis of patients with extreme neuropathic pain phenotypes, to determine the prevalence of gene variants associated with Neuropathic Pain Disorders, and to understand how the functional changes caused by gene variants relate to clinical presentation and neuropathic pain (supplementary figure 1).

Methods

Recruitment and clinical phenotyping of participants

We recruited patients with extreme neuropathic pain phenotypes, both sensory loss and gain, from secondary care clinics in the UK, located in Oxford, London, Salford, and Newcastle. Study participants with a history of lifestyle altering sensory disorder, either pain or loss of sensation, for greater than three months were invited to participate. The criteria for clinical case definitions are shown in table 1 (Turro *et al.*, 2020). We excluded patients with a known underlying genetic cause of chronic pain e.g. Fabry's disease and *SCN9A* congenital erythromelalgia (genetic pre-screening for these disorders was not mandatory), pregnancy, coincident major psychiatric disorders, poor or no English language skills, patients with documented central nervous system lesions, or patients with insufficient mental capacity to provide informed consent or to complete phenotyping. Description of the clinical phenotyping can be found in the summary NIHR Bioresource paper by Turro *et al.* (Turro *et al.*, 2020), and is briefly described here.

Study participants attended a single appointment that included a clinical assessment, screening for neuropathic pain, and specialised investigations to investigate for a distal symmetrical polyneuropathy. A detailed medical and drug history was taken, followed by a structured upper and lower limb neurological examination to detect clinical signs of a distal symmetrical polyneuropathy (Kleyweg *et al.*, 1991; Medical Research Council - Nerve Injuries Research Committee, 2010). DN4 questionnaire was used as a screening tool for neuropathic pain (Bouhassira *et al.*, 2005). Confirmatory tests included nerve conduction studies (England *et al.*, 2005), skin biopsy for intraepidermal nerve fibre density (Lauria *et al.*, 2010a; Lauria *et al.*, 2010b) and thermal thresholds in the area of neuropathic pain (Devigili *et al.*, 2019). Study participant's pain was assessed and graded (supplementary figure 2) according to published guidelines (Finnerup *et al.*, 2016).

Whole-blood samples were collected and sent to the NIHR BioResource laboratory in Cambridge. Detailed description of the DNA sequencing, WGS data-processing pipeline and identification of relevant gene variants can be found in Turro *et al.* (Turro *et al.*, 2020) and relevant aspects are summarised below.

All participants provided written informed consent in accordance with the Declaration of Helsinki. The study was approved by the East of England Cambridge South national research ethics committee (REC) reference 13/EE/0325.

Analysis plan

Genetic analysis was completed in two parts. The first analysis was to identify variants of clinical relevance in known pain genes. ~~The second was a gene wise association analysis,~~ grouping rare variants in genes for all neuropathic pain phenotypes considering both a targeted panel of pain genes and their promoters and all genes in the human genome that carried rare

1
2
3 variants. Two ion channel variants were selected for electrophysiological analysis to
4 investigate their functional impact (supplementary figure 1).
5
6

7 **Clinical reporting of pertinent findings**

8 *Gene list and transcript selection*

9
10 A list of genes separated into three tiers were curated at the time of recruitment in 2015 and
11 updated in 2021 (table 2). The division was based on the strength of evidence for the gene
12 being linked to neuropathic pain (Turro *et al.*, 2020). Only Tier 1 genes were discussed in the
13 multi-disciplinary team meetings and considered for clinical reporting.
14
15

16 *Variant filtering to identify variants of clinical relevance*

17 Variants of the 14 Tier 1 Neuropathic Pain Disorders genes were prioritised based on
18 (i) Minor Allele Frequency (MAF) in gnomAD < 1/1,000 if variant not previously described
19 in association with disease, or < 25/1,000 if the variant was present as disease-causing or
20 questionable disease-causing in Human Gene Mutation Database (HGMD).
21
22 (ii) predicted impact according to Ensembl Variant Effect Predictor ~~were~~ “High”,
23 “Moderate”, or “splice region variant”. Variants with more than three alternate alleles or an
24 internal MAF > 10% were discarded to guard against errors in repetitive regions and prevent
25 potential systematic artefacts (Turro *et al.*, 2020).
26
27
28
29

30 *Variant interpretation in multi-disciplinary teams meeting*

31 Prioritised variants were assessed by a multi-disciplinary team (Turro *et al.*, 2020).
32 Pathogenicity assignment was ascribed according to guidelines of The American College of
33 Medical Genetics (Richards *et al.*, 2015). Variants were classified as pathogenic, likely
34 pathogenic, variant of uncertain significance (VUS), likely benign, or benign. Clinically
35 relevant variants were those deemed medically actionable i.e. variants that could result in
36 specific, defined medical recommendations, and were reported to the referring clinician.
37 Pathogenic, and likely pathogenic variants were deemed clinically relevant.
38 VUS were deemed clinically relevant if:
39

- 40 1) *in vitro* functional studies showed that the variant altered function but the relationship to
41 clinical phenotype was not clear, particularly if a significant gene and environment interaction
42 was suspected; or
- 43 2) *in silico* analysis of the variant suggested a significant effect on function as defined by
44 - variant position: in a functionally important domain; located in a highly evolutionary
45 conserved section; significant biochemical consequences of amino acid exchange; affecting
46 protein structure.
47 - minor allele frequency
48 - concordant pathogenicity through multiple *in silico* algorithms such as SIFT, ~~P~~polyphen and
49 Align GDVD.
50

51 VUS that did not meet the above criteria, likely benign and benign variants were not reported.
52
53
54
55
56
57
58

59 **Group-wise Rare Variant Association Testing**

1
2
3 Genetic association testing in genes carrying rare variants was carried out using the gene-wise
4 approach of the combined burden and variance-component test SKAT-O (Lee *et al.*, 2012a;
5 Lee *et al.*, 2012b). The SKAT-O test combines a standard gene burden test that maximises
6 power under the assumption that all rare variants collapsed in a specific gene region are causal
7 and acting in the same direction towards the phenotype and the sequence kernel association
8 that calculates the weighted sum of squares of the variant score statistics and thus is more robust
9 to the presence of variants with opposing effects. The combined SKAT-O test calculates a
10 linear combination of the burden and variant-component test. Parametric bootstrap was used to
11 resample residuals under the null model. The same resampled bootstrap phenotypes,
12 considering covariates, were used for each gene. The weighting of the linear combination is
13 optimised from the data itself. The Rho statistic indicates the weighting of each test and gives
14 an indication of the causality and directionality of the variants' effects, with rho=1 reducing
15 SKAT-O to a burden test (high percentage of causality in the same direction) and a rho=0 to a
16 SKAT (causal and non-causal variants with opposing directions). Age, sex and the three first
17 Principal Components of genetic variation were used as covariates. Only un-related individuals
18 were used in the group-wise rare-variant analysis. Analysis was done per ethnicity and
19 neuropathic pain clinical phenotype.
20
21
22
23
24
25

26 27 *Data filtering and pre-process*

28 Only participants with neuropathic pain were included for gene-wise rare variant association
29 testing. In total 39 participants were excluded from the original cohort of 205 for the SKAT-O
30 analysis (8 with no neuropathic pain; 2 age not available; 7 sequencing by Genomics England
31 not available as mapped to Grch38 genome assembly and joint genotyping not conducted; 4 as
32 only founders from families included). Exclusions were also based on ethnicity. We only
33 considered 128 Europeans and 38 Africans with neuropathic pain as cases, 4 South-Asians and
34 14 people of "Other" ethnicity were not included. Unrelated individuals from the NIHR-
35 Bioresource Rare Diseases cohort, not recruited as a part of Neuropathic Pain Disorders nor
36 the Neuro Developmental Disorders cohort, were included as controls. Analysis for individuals
37 with European and African ethnic origin were separated. The sample size used was 128
38 Europeans and 38 Africans as cases versus 5945 and 154 as ethnically matched controls
39 respectively.
40
41
42
43
44

45 VCF files were normalised, left aligned and multi-allelic SNPs were broken down to bi-allelic
46 using BCF-tools. Only SNPs and indels that were rare in gnomAD (MAF < 0.001), not
47 common in the whole NIHR Bioresources Rare Diseases cohort (MAF < 0.05), and had MAF
48 < 0.05 in cases and controls combined for each phenotype were considered. Variants should
49 have passed the quality filters in the joint genotyping calls and be of high quality with a call
50 rate > 99%, following HWE equilibrium (p value > 0.05). Alleles should have high average
51 base call depth (> 10) and average genotype quality (> 20). Regulatory regions for Tier1-3
52 genes were downloaded using the GeneHancer resource from GeneCards. We then selected
53 regions annotated as promoters or promoters/enhancers for the Tier 1-3 genes and were
54 collapsed in one group associated with the respective gene. For the panel of Tier1-3 genes and
55 their promoters we considered variants with "modifier", "moderate" and "high" impact effects.
56 We further selected variants that were Nonsynonymous or having the EPACTS functional
57
58
59
60

1
2
3 annotations: Essential_Splice_Site, Normal_Splice_Site, Start_Loss, Stop_Loss, Stop_Gain,
4 5' UTR and 3' UTR. For the whole gene set (all genes in the human genome), we only
5 considered variants of “moderate” or “high” Variant Effect Predictor impact on protein coding
6 genes. Manta and Canvas software packages were used for detection of deletions >50 b pas
7 described previously (Turro *et al.*, 2020). Due to the limited sample size and multiple sub-
8 phenotypes we focused on protein coding genes and high and moderate impact variants for the
9 whole gene set analysis.
10
11
12

13
14 Separate analysis was completed for: 36 Tier 1-3 genes (72 groups with their respective
15 promoters); functionally validated variants in three voltage-gated sodium channels *SCN9A*,
16 *SCN10A*, and *SCN11A* (Bennett *et al.*, 2019); and the whole gene set (approximately 20000
17 genes).
18
19

20 **Functional *in vitro* studies of *SCN9A* [p.Arg185HisR185H](#) and *TRPA1* [p.Ala172Val](#)** 21 **variants**

22 *Plasmids and site-directed mutagenesis*

23
24 Human Na_v1.7 cDNA was cloned into a modified pcDNA3 expression vector containing
25 downstream IRES and dsRED2 sequences (*SCN9A*-IRES-DsRED). Human β1 and β2 subunits
26 were cloned into pIRES2-AcGFP (*SCN1B*-IRES-*SCN2B*-IRES-eGFP)(Cox *et al.*, 2006).
27 Human TRPA1 cDNA was cloned into a modified pcDNA3 expression vector containing
28 downstream IRES and dsRED2 sequences (*TRPA1*-IRES-DsRED) (Cox *et al.*, 2006). The
29 mutations [p.Arg185HisR185H](#), [p.Ala172ValA172V](#) and [p.AsnN855Ser](#) were introduced using
30 QuickChange II XL site-directed mutagenesis kit (Agilent). The clones were sequenced by
31 standard methods.
32
33
34
35

36 *HEK293T cell culture and transfection*

37
38 Human embryonic kidney HEK-293T cells were grown in a Dulbecco's modified Eagle's
39 culture medium (DMEM/F-12, Invitrogen) containing 10% fetal bovine serum and maintained
40 under standard conditions at 37 °C in a humidified atmosphere containing 5% CO₂. For study
41 of the *SCN9A*(*ENST00000409672.1*):c.554G>A, [p.Arg185HisR185H](#) variant, cells were
42 transfected using the jetPEI™ transfection reagent (Polyplus-transfection Inc.) with either WT
43 or mutant Na_v1.7 channel combined with β1 and β2 subunits (2:1 ratio). For study of
44 *TRPA1*(*ENST00000262209.4*):c.515C>T, ~~[p.A172V](#)~~ [p.Ala172Val](#) and
45 *TRPA1*(*NM_007332.3*):c.2564A>G, ~~[p.N855S](#)~~[p.Asn855Ser](#) variants, cells were co-transfected
46 with pMaxGFP (Amaxa) and either human *TRPA1* wild-type or human *TRPA1*-[p.Ala172Val](#)
47 [A172V](#)/[p.AsnN855Ser](#) at a ratio of 1:5 to facilitate visualisation of positively transfected cells.
48 The total amount of plasmid DNA transfected was 1.2 µg/µl per 35 mm dish. pMaxGFP
49 positive cells were used as control. Cells were used 36 to 72 hours after transfection.
50 Experiments were performed at room temperature, and repeated on three or more separate
51 transfections.
52
53
54
55
56

57 *Electrophysiology*

58
59 Voltage clamp experiments were performed on transfected HEK293T cells. Whole-cell patch
60 clamp recordings were conducted using an Axopatch 200B Amplifier, the Digidata 1550B Low

Noise Data Acquisition System and the pClamp10.6 software (Molecular Devices). Data were filtered at 5kHz and digitized at 20kHz. Capacity transients were cancelled, and series resistance compensated at 70-90% in all experiments. Cells were continuously superfused with extracellular solution or agonist-containing solutions through a common outlet. Standard extracellular solutions for the patch clamp experiments were used to study the respective *SCN9A* (Blesneac *et al.*, 2018) and *TRPA1* (Kremeyer *et al.*, 2010; Avenali *et al.*, 2014b) variants.

Electrophysiology study of SCN9A p.Arg185HisR185H

The extracellular solutions contained (in mM): 140 NaCl, 3 KCl, 1 CaCl₂, 1 MgCl₂, 10 HEPES, pH 7.3 with NaOH (adjusted to 320 mOsm/L with glucose). Patch pipettes were filled with an internal solution containing (in mM) 140 CsF, 10 NaCl, 1 EGTA, 10 HEPES, pH 7.3 with CsOH (adjusted to 310 mOsm/L with glucose) and had a typical resistance of 2-3MΩ. Leak currents were subtracted using a P/5 protocol, applied after the test pulse. A holding potential of -100mV and an intersweep interval of 10s was used for all the protocols. Measurements were done at 10°C, 20°C and 30°C.

Electrophysiology studies of TRPA1 p.Ala172ValA172V and p.Asn855SerN855S variants

To study the effects of agonist-desensitization on channel activation, the extracellular solution contained (in mM): 127 NaCl, 3 KCl, 1 MgCl₂, 10 HEPES, 2.5 CaCl₂, and 10 glucose, pH 7.4 with NaOH. Osmolarity was adjusted to 310 mOsm/L with glucose. The intracellular solution contained (in mM): 135 KCl, 2 MgCl₂, 2 MgATP, 5 EGTA, and 10 HEPES, pH 7.4 with CsOH. Osmolarity was adjusted to 300 mOsm/L with glucose (Avenali *et al.*, 2014a).

To study the effects of intracellular calcium in channel modulation, the extracellular solution contained (in mM): 140 NaCl, 4 KCl, 2 CaCl₂, 1 MgCl₂, 10 HEPES, pH 7.4 with NaOH. Osmolarity was adjusted to 310 mOsm/L with glucose. The intracellular solution contained (in mM): 130 KCl, 8 NaCl, 2 EGTA, 1 MgCl₂, 1 CaCl₂, 4 MgATP, 0.4 Na2GTP, pH 7.4 with CsOH. Osmolarity was adjusted 300 mOsm/L with glucose.

To investigate voltage-dependence, currents were recorded during a voltage step protocol consisting of 400ms voltage steps to test potentials ranging from -100mV to +180mV, followed by a final invariant step to -75mV (400ms) to measure tail currents. The holding potential was set at -0mV.

The voltage-dependence activation of hTRPA1 p.Ala172ValA172V in response to mustard oil (Allyl isothiocyanate, AITC, a TRPA1 electrophilic agonist) and Menthol (non-electrophilic agonist of TRPA1) was measured. These recordings were performed in calcium-containing extracellular solution, to preserve agonist desensitization properties (Macpherson *et al.*, 2007). Perfusion with TRPA1 agonists was performed through a custom-made gravity perfusion system. Immediately after establishing the whole-cell configuration, perfusion was switched to extracellular solution for 2 min before beginning the voltage clamp recording. AITC (Sigma 377430) was dissolved in DMSO (Sigma D2650), and Menthol (Sigma M2772) in ethanol. The maximum final concentration of either DMSO or ethanol did not exceed 0.1%. The effect

of TRPA1 agonists on current-voltage curves were measured with a two voltage-step protocol, as described above. Voltage-ramps ranging from -100mV to + 100mV for 500ms, every 5 seconds, were applied to elucidate the temporal activation of hTRPA1 [p.Ala172ValA172V](#) in response to AITC. In this case, the holding potential was set at -70mV.

Current voltage curves (I-V curves) were fitted using a combined Boltzmann and linear ohmic relationship: $I/I_{\max} = G_{\max} (V_m - E_{\text{rev}}) / (1 + \exp^{(V_{1/2} - V_m)/k})$. Normalized conductance-voltage curves (activation curves) were fitted with a Boltzmann equation $G/G_{\max} = 1 / (1 + \exp^{(V_{1/2} - V_m)/K})$ where G was calculated as follows $G = I / (V_m - E_{\text{rev}})$. Steady-state fast inactivation curves were fitted with $I_T/I_{T\max} = 1 / (1 + \exp^{-(V_{1/2} - V_m)/k})$. Tail current derived voltage activation curves were fitted to the Boltzmann equation: $I_T/I_{T(\text{Max})} = 1 / (1 + \exp^{[(V_m - V_{1/2})/k]})$. In all the equations $V_{1/2}$ represents the half-activation and half inactivation membrane potentials; V_m is the membrane potential, E_{rev} the reversal potential, k the slope factor, G the conductance and I_T the current at a given V_m ; G_{\max} and $I_{T\max}$ are the maximum conductance and current respectively; R_{in} is the fraction of channels that are resistant to slow inactivation. Statistical significance was set at $p = 0.05$ for group comparisons.

Statistical analysis

Electrophysiology data are presented as mean \pm SEM. Statistical analysis for group comparisons included: Two-way ANOVA (temperature and genotype as categorical variables) for [p.Arg185His](#), and One-way ANOVA (genotype as categorical variable) for [p.Ala172Val](#) with Sidak's multiple comparison test. Statistically significant differences were defined $p < 0.05$. Frequencies of individual genetic variants were compared across groups using a two-tailed Fisher's exact test. Significance for gene-wise associations was set to the Bonferroni adjusted 0.01 threshold for the number of genes considered. Unadjusted p values are reported alongside the significance threshold.

Data availability

The genotype and phenotype data can be accessed by application to the NIHR BioResource Data Access Committee at dac@bioresource.nihr.ac.uk or by application to Genomics England Limited following the procedure outlined at <https://www.genomicsengland.co.uk/about-gecip/joining-researchcommunity/>.

Results

Study participants

A total of 205 study participants with extreme phenotypes were included (figure 1). Age ranged 4.8-84.3 years, and 115 (~~55.1~~56.1%) participants were men and 90 (43.9%) were women. In total 38* participants were recruited of African descent. The majority of participants (90.2%) satisfied criteria for probable or definite chronic neuropathic pain. Participants with possible neuropathic pain (5.9%) included those with “neuropathic-type” pain (burning, stabbing, electric like shocks, dysaesthesias) in a neuroanatomically plausible distribution, but with no evidence of nerve injury on clinical examination or specialised investigations. Examples include those with episodic pain syndromes or those with burning pain of the hands and feet with a normal clinical examination and investigations. A group of participants (8, 3.9%) did not experience neuropathic pain, including participants with loss of pain sensation.

Gene variants reported – Tier 1 gene analysis.

After multi-disciplinary team discussion, 26 (12.0%) gene variants were categorised as clinically relevant: 3 pathogenic (1.4%), 2 likely pathogenic (0.9%) and 21 VUS deemed relevant for reporting (9.7%). Apart from three participants who declined consent for feedback of genetic testing, all variants were reported to the referring clinician. The results are summarised in table 3.

Three participants were diagnosed with pathogenic mutations. Two sisters with severe erythromelalgia, present since childhood, have the same pathogenic variant in *SCN9A* p.R1848Tp.Ile848Thr. This variant is not present in control populations, is reported in several inherited erythromelalgia pedigrees, and causes gain of function through a hyperpolarising shift in the voltage dependence of activation (Cummins *et al.*, 2004; Yang *et al.*, 2004). A pathogenic variant in *SPTLC1* p.C133Wp.Cys133Trp was identified in a participant diagnosed with a painful sensorimotor neuropathy, and is the commonest pathogenic *SPTLC1* mutation causing hereditary sensory neuropathy type-1 identified in UK patients (Davidson *et al.*, 2012).

Two participants diagnosed with small fibre neuropathy carried likely pathogenic variants, *SCN10A* p.G1662Sp.Gly1662Ser and *SCN11A* p.C1543Yp.Cys1543Tyr. This conclusion was based on criteria available at the time of interpretation, low frequency in genetic databases, location in important region of the channel, high probability of affecting channel function and previous description in small fibre neuropathy (Faber *et al.*, 2012a); however, we note that this variant is classified as likely benign in ClinVar. The remaining 21 variants reported were classified as VUS, due to our conservative approach in assigning pathogenicity.

Of the 40 participants recruited with non-freezing cold injury, six participants (7.5% allele frequency) carry the *SCN9A* p.R185Hp.Arg185His variant, which is associated with small fibre neuropathy (Faber *et al.*, 2012a; Han *et al.*, 2012). The six participants were all of African descent (the majority from Ghana). Chronic non-freezing cold injury is an acquired painful sensory neuropathy observed almost exclusively in soldiers (Vale *et al.*, 2017). Soldiers of

1
2
3 African descent are disproportionately affected when compared to Caucasian soldiers. The
4 allele frequency of p.Arg185His p-R185H-variant is less than 1% in gnomAD (1.4% in the
5 African/African-American population); 165 individuals carried the allele in general gnomAD
6 population, 125 of which were Africans (166 allele counts, 1 was homozygote). Within NIHR
7 Bioresource controls of African ancestry, p.Arg185His p-R185H-allele frequency was 0.0065
8 (2 out of 104 participants, 1.3%). In our cohort (figure 2a), the allele was significantly more
9 common (6 out of the 38 participants) compared to both the general gnomAD population
10 (Fisher's Exact test, P value = 1.4×10^{-7} , OR = 28.17, 95%CI [9.98, 65.45]), the gnomAD
11 African population (Fisher's Exact test, P value = 0.001, OR = 5.66, 95%CI [2, 13.03]), and
12 NIHR Bioresource African controls (Fisher's Exact test, P value = 7.6×10^{-4} , OR = 13.68,
13 95% CI [2.41, 143.26]).

14
15
16
17
18
19 The variant, p.Arg185His p-R185H, results in an amino acid substitution in the linker between
20 D1/S2 and D1/S3, which lies within a voltage sensing domain of Na_v1.7 (figure 2b). This
21 residue is highly conserved across all voltage-gated sodium channels. ~~The amino acid~~
22 ~~substitution is predicted to be “probably damaging” and “deleterious” according to the *in silico*~~
23 ~~tools Polyphen and SIFT.~~ Functional studies have shown that p.Arg185His p-R185H-variant
24 does not alter channel gating properties at room temperature; however, it was associated with
25 enhanced resurgent currents, and increases excitability when expressed in dorsal root
26 ganglion neurons (Han *et al.*, 2012).

27
28
29
30
31 Intronic variants and the detection of deletions were included in the gene level analysis, and
32 none were deemed medically actionable or of interest.

33 34 35 **The impact of *SCN9A* p-R185H p.Arg185His variant on Na_v1.7 channel function is** 36 **temperature dependent**

37
38 Non-freezing cold injury is caused by cold environmental exposure and neuropathic pain is
39 worsened by further cold exposure. We hypothesised that there may be an interaction between
40 Na_v1.7 and an environmental trigger, such that cooling magnifies the effect of
41 p.Arg185His p-R185H-variant on channel function. Wild type (WT) and p.Arg185His p-R185H
42 Na_v1.7 channels were expressed in combination with β1 and β2 subunits in HEK293T cells
43 and Na_v1.7 mediated currents recorded by whole cell patch clamp (Figure 2c-h). Changing the
44 temperature from 20°C to 10°C did not significantly affect the half-activation potential of
45 p.Arg185His p-R185H (Figure 2c), but significantly shifted the half-inactivation potential for
46 steady-state fast inactivation of p.Arg185His p-R185H-mutant compared to WT (figure 2d).
47 Channel kinetics were slower at 10°C compared to 20°C with similar effects for WT and
48 p.Arg185His p-R185H (Figure 2e). We also wanted to assess channel behaviour at higher
49 temperatures (30°C). Increasing the temperature from 20°C to 30°C did not affect I-V curve or
50 the steady-state inactivation of the WT or the p.Arg185His p-R185H (Figure 2 f, g). Faster
51 inactivation kinetics were observed at 30°C and the change was similar for WT and p-R185H
52 p.Arg185His (Figure 2h).

In conclusion, the [p.R185H](#) [p.Arg185His](#) mutant exhibited a depolarising shift of half-inactivation potentials at 10°C but not at 20°C or 30°C, which is a change in channel gating consistent with gain of function only at lower temperatures.

Gene-wise Rare Variant Association Testing Results

When comparing European participants against controls, gene-wise, rare variant association testing for Tiers 1-3 genes identified six genes and regulatory regions of 4 genes with significant difference in rare variant distribution (table 4). In total, 177018 genomic loci were called in Tier 1-3 genes, 132605 SNPs (93295 were singletons), 4059 insertions and 8498 deletions (8859 out of the 12557 were singletons). Variants per loci rate was 0.000046 in priority genes regions. Heterozygosity to Homozygosity ratio was 0.96, 1.35 for SNPs and 0.29 for INDELS. For European participants, gene-wise rare variant association varied according to clinical phenotype (supplementary table 1), and 20 genes and 24 regulatory regions reached Bonferroni adjusted significance for at least one phenotype. For African participants several genes showed similar associations with post-traumatic neuropathy, small fibre neuropathy and non-freezing cold injury (supplementary table 1).

For the groups of functionally validated voltage-gated sodium channel variants, a significant association of *SCN10A* with small fibre neuropathy in Europeans was found. This was driven by two gain of function variants, *SCN10A(ENST00000449082.2):c.4984G>A*, [p.Gly1662Sp-G1662S](#) (Allele frequency 0.0039 in Neuropathic Pain and 0.0005 in controls) and *ENST00000449082.2:c.1661T>C*, [p.L554P-p.Leu554Pro](#) (Allele frequency 0 in Neuropathic Pain and 0.00008 in controls) (Table 4). These variants are reported in patients with small fibre neuropathy, cause gain of function of the $Na_v1.8$ channel and enhance dorsal root ganglion neuron excitability (Faber *et al.*, 2012b; Han *et al.*, 2014). However, both variants were characterised as likely benign in ClinVar and their allele frequencies in gnomAD suggest that they cannot be the only cause of neuropathic pain. No significant associations were found for *SCN9A*, nor *SCN11A*.

For the whole gene set analysis, 146 genes reached Bonferroni corrected significance in Europeans with neuropathic pain when compared to controls (supplementary table 2). Four of the genes, *KIF1A*, *KCNQ5*, *KCNK4* and *NOS2* are linked to human neuropathic pain.

The *TRPA1* [p.A172V](#) [p.Ala172Val](#) variant is associated with episodic pain and gain of channel function

Variants in Tier 2 and 3 genes were filtered, using the same approach as for Tier 1 genes to identify those that may be pathogenic. A rare *TRPA1* variant, [p.A172V](#) [p.Ala172Val](#) (gnomAD allele frequency 0.0003), was identified in a participant who suffers from episodic widespread chronic pain with neuropathic characteristics particularly affecting the trunk. Clinical phenotype was similar to a neuropathic pain syndrome associated with a *TRPA1* channelopathy ([p.N855S](#) [p.Asn855Ser](#) variant) (Kremeyer *et al.*, 2010); however, the participant's pain was not precipitated by physiological stressors. MRI of the brain and spine, nerve conduction studies and skin biopsy of the lower leg were within age and gender appropriate reference ranges. The participant's child, carrying the same variant, was similarly affected by chronic

1
2
3 abdominal and pelvic pain with normal investigations. *In silico* tools, PolyPhen and SIFT
4 scores, predicted [p.A172V](#) [p.Ala172Val](#) to be deleterious. The variant is moderately conserved
5 across species (Figure 3a), is situated within the ankyrin repeat domain of the protein (Figure
6 3b) and is a non-polar to non-polar amino acid exchange (Grantham score 64). Based on the
7 rarity of the variant, clinical phenotype consistent with the TRPA1 Familial Episodic Pain
8 Syndrome, positive family history and *in silico* analysis showing the variant to be in the poorly
9 understood N-terminal ankyrin repeats, the *TRPA1* [p.Ala172Val](#) [p.A172V](#) variant was
10 prioritised for functional studies. These were compared to the *TRPA1* variant [p.N855S](#)
11 [p.Asn855Ser](#) which is the only variant previously linked to this disorder.

12
13
14
15
16 The biophysical properties of WT, [p.Ala172Val](#) [p.A172V](#) and [p.N855S](#) [p.Asn855Ser](#) hTRPA1
17 were compared (supplementary figure 3). In HEK293T transfected cells, TRPA1 current-
18 voltage relationship and half-maximal activation for WT, [p.A172V](#) [p.Ala172Val](#) and [p.N855S](#)
19 [p.Asn855Ser](#) were not statistically different. Under control conditions WT, [p.A172V](#)
20 [p.Ala172Val](#) and [p.N855S](#) [p.Asn855Ser](#) current traces showed sustained outward rectification
21 at positive potentials, consistent with an underlying voltage dependence of channel gating. As
22 current density did not differ between WT and the variants, under control conditions, it is
23 unlikely that channel trafficking is affected in [p.A172V](#) [p.Ala172Val](#) and [p.N855S](#)
24 [p.Asn855Ser](#) channels.

25
26
27
28
29 Voltage-dependence activation of hTRPA1 [p.A172V](#) [p.Ala172Val](#) and [p.N855S](#) [p.Asn855Ser](#)
30 was measured in response to mustard oil (Allyl isothiocyanate, AITC, a TRPA1 electrophilic
31 agonist) and Menthol (non-electrophilic agonist of TRPA1). In response to 25 μ M AITC, in
32 the presence of extracellular calcium, [p.A172V](#) [p.Ala172Val](#) showed a pronounced
33 linearisation of the current-voltage relationship compared to WT in response to a two voltage-
34 step protocol. A steeper activation curve was observed at positive potentials for both
35 [p.Ala172Val](#) [p.A172V](#) and [p.N855S](#) [p.Asn855Ser](#) compared to WT (Figure 3c). Currents were
36 significantly increased at positive potentials for [p.A172V](#) [p.Ala172Val](#) (Figure 3d) and at
37 negative potentials for [p.N855S](#) [p.Asn855Ser](#) (Figure 3e). Analysis of tail currents
38 demonstrated a significant leftward shift of voltage dependence of channel activation in the
39 presence of AITC for both variants (Figure 3f); however, the slope of the voltage-activation
40 curve did not significantly change. Current-voltage relationships, tested with a voltage-ramp
41 protocol, showed an increase in current densities at positive potentials after application of
42 25 μ M AITC (figure 3g). In summary, these findings show an enhanced response of [p.A172V](#)
43 [p.Ala172Val](#) to 25 μ M AITC, suggesting a gain-of-function behaviour of this variant, under
44 agonist stimulation.

45
46
47
48
49
50
51
52 Application of 100 μ M Menthol did not significantly change current density nor voltage
53 sensitivity when applied to [p.A172V](#) [p.Ala172Val](#) or [p.N855S](#) [p.Asn855Ser](#) in the presence of
54 extracellular calcium (supplementary figure 4). However, in the presence of both extracellular
55 and intracellular calcium, significant changes were observed (Figure 4a-d). Both [p.A172V](#)
56 [p.Ala172Val](#) and [p.N855S](#) [p.Asn855Ser](#) channels showed an increase in outward currents and
57 voltage sensitivity in response to 100 μ M Menthol.

1
2
3 | In summary, the ~~p.A172V~~ p.Ala172Val variant confers gain of function properties on TRPA1
4 channel in response to the agonists AITC and Menthol. For the latter, the effect was dependent
5 on intracellular calcium.
6
7
8
9
10
11
12
13
14
15
16
17
18
19
20
21
22
23
24
25
26
27
28
29
30
31
32
33
34
35
36
37
38
39
40
41
42
43
44
45
46
47
48
49
50
51
52
53
54
55
56
57
58
59
60

For Review Only

Discussion

In this study we applied whole genome sequencing to a cohort of patients with Neuropathic Pain Disorders. We carried out two analyses. First, we identified medically actionable variants and second, we carried out group-wise associations tests at the gene level for rare variants. The diverse phenotypes ranged from congenital insensitivity to pain to painful neuropathy. Clinically relevant findings in genes associated with pain were reported in 12% of participants. The majority of clinically relevant variants were in voltage-gated sodium channels. We made new genotype-phenotype associations, such as the Nav1.7 [p.R185Hp.Arg185His](#) variant which was more frequent in Africans with non-freezing cold injury. We provide new mechanistic insights showing that [p.R185Hp.Arg185His](#) interacts with cold, causing gain of function in the Nav1.7 gating properties. The gain of function of [p.A172V](#) [p.Ala172Val](#) in TRPA1 in response to agonists extends our knowledge of painful TRPA1 channelopathies.

The study of genetic neuropathic pain disorders poses challenges in describing clinical phenotype and assigning pathogenicity to associated variants. We used the gold standard grading system, of the Neuropathic Pain Special Interest Group of IASP (Finnerup *et al.*, 2016). Such an approach works well in disorders where there is structural injury to sensory neurons. For example, in painful distal symmetrical polyneuropathy, pain and sensory signs are found in a neuroanatomically plausible distribution (meeting probable criteria), and specialised investigations confirm a lesion of the somatosensory nervous system (meeting definite criteria). However, the majority of Mendelian pain disorders are sensory neuron ion channelopathies, in which pain is episodic, with no structural injury to sensory neurons. For example, in Inherited Erythromelalgia (Nav1.7) or Familial Episodic Pain Syndrome (TRPA1, Nav1.9), sensory examination (between pain episodes), neurophysiology and cutaneous innervation are normal. Careful attention to clinical history is therefore essential.

We identified medically actionable variants in 12% of the participants. In our cohort, five participants carry ~~clear~~/[pathogenic or](#) likely pathogenic variants. Four pathogenic variants were in voltage-gated sodium channels, which can impact patient care. For example, a pair of sisters with Inherited Erythromelalgia carry the pathogenic *SCN9A* [p.Ile848Thrp.I848T](#)—with autosomal dominant pattern of inheritance. Only a minority of patients with Inherited Erythromelalgia possess *SCN9A* mutations (Zhang *et al.*, 2014). Identification of a genetic cause for erythromelalgia means family genetic counselling and preferential treatment with non-selective sodium channel blockers (Cregg *et al.*, 2014), which is not the standard treatment for other causes of neuropathic pain (Finnerup *et al.*, 2015). The family may also access future treatments such as selective sodium channel blockers (Alsaloum *et al.*, 2020).

A further 20 participants carry VUS in voltage-gated sodium channels that were deemed clinically relevant. Ascribing pathogenicity to ion channel variants is difficult. The majority are relatively common, exhibit subtle channel gain of function effects and likely interact with environmental factors. For example, in our cohort the *SCN9A*(*ENST00000409672.1*): [c.2215A>G](#), [p.Ile739Valp.I739V](#)—variant was found in four participants with painful

1
2
3 neuropathy and described previously as pathogenic (Han *et al.*, 2012). However,
4 [p.Ile739Valp.I739V](#) is common in the general population (0.2% allele frequency), while the
5 prevalence of small fibre neuropathy is rare (approximately 50 per 100 000 (Peters *et al.*,
6 2013)). It is unlikely that this variant is fully penetrant (thus pathogenic); but may act as a risk
7 factor. Nevertheless, it is important to identify such variants for treatment selection, because
8 Lacosamide (a sodium channel blocker) has shown efficacy in a clinical trial of patients with
9 small fibre neuropathy and rare *SCN9A* (de Greef *et al.*, 2019) variants. Voltage clamp analyses
10 can add valuable experimental evidence to the pathogenicity assessment that cannot be
11 replaced by in-silico prediction tools ~~The gold standard remains electrophysiological analysis,~~
12 as *in silico* analysis is not comprehensive and variant's effect prediction software are likely to
13 underestimate the impact of the gain-of-function effects. ~~;~~ ~~H~~ However, recent advances in ion
14 channel modelling has improved outcomes (Heyne *et al.*, 2020).

20 Whole genome sequencing is now integrated into the UK national health system (see
21 <https://www.genomicsengland.co.uk/>) and is now considered standard of care across the UK
22 (The 100000 Genomes Project Pilot Investigators, 2021). As of 2022 all testing at NHS
23 genomic centres for painful neuropathies and channelopathies is via whole genome sequencing.
24 The panel application 'Inherited neuropathies or pain disorder v1.36' was informed by the
25 NIHR Bioresource, (100,000 genomes) ~~and~~ our functional studies and includes all the tier 1
26 pain genes in this paper ~~as well as~~ ~~and~~ *TRPA1*. Such an approach will identify many more new
27 variants and the findings of our study will be of direct relevance to practitioners assessing
28 patients with neuropathic pain. Understanding how these novel variants relate to clinical
29 phenotype presents significant challenges for clinicians. The combined expertise of our
30 multidisciplinary teams meetings were vital in the interpretation of variant pathogenicity.
31 ~~Therefore, the findings of our study will be of direct relevance to practitioners assessing
32 patients with neuropathic pain.~~ We note that the proportion of cases in which we have found a
33 pathogenic variant that explains the clinical pain phenotype was low (2.4%), although in a
34 higher proportion (a further 10%) the finding was clinically actionable. In many cases this was
35 VUS in which the relationship to the clinical phenotype could not be causally established; but
36 could still have implications for treatment and so was reported. The low yield in solving cases
37 at a diagnostic level partly represents the fact that neuropathic pain is monogenic in only a
38 minority of cases. In many cases it is likely to arise from gene-environment interaction and/or
39 multiple genes. To try and improve diagnostic yield in the future we could enrich analysis
40 pipelines (for instance to include analysis of repeat expansions in the WGS data), expand co-
41 segregation analysis and also functional analysis. It is not possible to test all novel variants
42 with current patch clamp technology. ~~Automated prediction of pathogenicity and higher
43 throughput functional assays should be a priority, and important next steps in the integration
44 of whole genome sequencing into healthcare.~~

52 We were able to extend genotype-phenotype associations of *SCN9A*. The *SCN9A*
53 [p.R185Hp.Arg185His](#) variant was more common in study participants with non-freezing cold
54 injury. [p.R185Hp.Arg185His](#) is associated with neuropathic pain disorders, such as small fibre
55 neuropathy (Faber *et al.*, 2012a) and painful diabetic neuropathy (Blesneac *et al.*, 2018). Non-
56 freezing cold injury is a chronic neuropathic pain disorder caused by an acquired sensory
57 neuropathy (Vale *et al.*, 2017) after prolonged exposure to cold and wet environments. Further
58
59
60

1
2
3 cold exposure intensifies the neuropathic pain in a similar manner to cold allodynia after
4 platinum based chemotherapy (Benedsgaard *et al.*, 2020). The mechanism for this cold
5 allodynia is unknown. We show that [p.R185Hp.Arg185His](#) displays gain of function
6 characteristics at lower temperatures. This occurs through a shift of fast inactivation at 10°C,
7 but not at 30°C or room temperature (20°C). Pathogenic *SCN9A* variants that cause inherited
8 erythromelalgia demonstrate temperature sensitivity at biophysical and clinical level such that
9 warming intensifies pain and cooling is analgesic (Han *et al.*, 2007). A link therefore exists
10 between biophysical properties of Na_v1.7 channel, clinical phenotype and temperature
11 sensitivity. An increase of [p.R185Hp.Arg185His](#) variant excitability on cooling may contribute
12 to cold allodynia in a sub-group of non-freezing cold injury patients. Another consideration is
13 that increased activity of [p.R185Hp.Arg185His](#) at cold temperatures could injure nerves
14 through calcium dependant excitotoxicity (Hoeijmakers *et al.*, 2012; Estacion *et al.*, 2015). [In
15 summary, p.Arg185His may contribute to clinical phenotype or increase risk for cold induced
16 neuropathic pain; but, we cannot conclude that is causative in in isolation.](#)
17
18
19
20
21
22

23 Bevimed is an inference procedure for identifying loci associated with rare hereditary disorders
24 using Bayesian model comparison, and was used in an analysis of all cohorts of NIHR
25 BioResource Rare Diseases (Turro *et al.*, 2020). Under different modes of inheritance there
26 was strong evidence for 95 genes and 29 binary disease tags (cases versus controls). No
27 diseases from our cohort were amongst the associations with strong evidence. We used SKAT-
28 O in our cohort. Group-wise association tests can increase the power to detect associations
29 between rare alleles and phenotypes by aggregating variant counts on the gene level that can
30 have an impact on gene function. Neuropathic pain can arise as a complex effect of rare variants
31 with causal effects in the same direction, which the burden test is best powered to detect, or
32 effects with different levels of causality and direction, which the sequence kernel association
33 test is best powered to detect. We used an approach that maximises test power by considering
34 the combination of both the burden and sequence kernel association tests. In testing for
35 associations for the whole gene set in Europeans with neuropathic pain, 146 genes reached
36 statistical significance. These are gene-wise results showing a significant association of a
37 configuration of rare alleles grouped at the gene level with certain neuropathic pain phenotypes.
38 In most of the associations, the variant component test was better powered. This is indicated
39 by the low Rho statistics empirically calculated from the data, and is suggestive of the presence
40 of variants with different values of causality and opposing direction of effects towards the
41 phenotype, i.e. both protective and deleterious variants present and driving the association. We
42 focused on bi-allelic variants and indels of high quality, with moderate to high impact on
43 protein coding genes, as we had a moderate sample size and did not want to diminish statistical
44 power after Bonferroni correction. The genes *KCNK4*, *KCNQ5* and *NOS2*, were significantly
45 associated with neuropathic pain after gene-wise rare variant association testing, These have
46 not been previously linked to human pain at a genetic level; but, preclinical models have
47 implicated these genes in pain pathogenesis (Noël *et al.*, 2009; Liu *et al.*, 2021; Shnayder *et*
48 *al.*, 2021). *KIF1A*, a Tier 2-3 priority gene also reached genome wide significance. The
49 association with neuropathic pain would require replication in independent cohorts and
50 functional studies.
51
52
53
54
55
56
57
58
59
60

1
2
3 We undertook an analysis focusing on genes known or likely to be implicated in neuropathic
4 pain, and we therefore used more relaxed criteria in filtering rare variants, including modifier,
5 moderate and high impact variants. We also note that as our *in silico* variant effect predictions
6 are limited by their tendency to under-estimate gain of function effects. Our analysis showed
7 an association of five Tier 2 genes, including *TRPA1*, with neuropathic pain. TRPA1 is a
8 calcium permeable non-selective cation channel that acts as a sensor of noxious external
9 stimuli, such as mustard oil (AITC) and Menthol. The [p.N855Sp.Asn855Ser](#) TRPA1 variant
10 is associated with familial episodic pain syndrome characterised by truncal pain triggered by
11 physiological stress or exercise (Kremeyer *et al.*, 2010). We identified a study participant with
12 a similar clinical phenotype of truncal pain who carried the [p.A172V-p.Ala172Val](#) TRPA1
13 variant. [p.A172V-p.Ala172Val](#) is a missense mutation in the fourth domain of the Ankyrin
14 region. Our *in vitro* electrophysiological studies show that TRPA1 [p.A172V-p.Ala172Val](#)
15 variant causes gain of function in response to agonist stimulation, and provides evidence for
16 Ca²⁺-mediated channel activation through the Ankyrin repeat domains of TRPA1 channel.
17
18
19
20
21
22

23 TRPA1 consists of a large intracellular NH2 and COOH termini, with the NH2 terminus
24 containing an elongated ankyrin repeat domain which is highly conserved. Human TRPA1
25 consists of 16 ankyrin repeat domains that connects to the transmembrane domains *via* a linker
26 region. The [p.A172V-p.Ala172Val](#) variant did not change the biophysical properties of TRPA1
27 channel in the naïve state, but did enhance responses to AITC and Menthol. Current density
28 was larger for AITC when compared to Menthol. Due to difference in their electrophilic nature,
29 agonists vary in their ability to covalently (AITC) or noncovalently (Menthol) modify the
30 channel upon binding. This difference in channel binding might underlie different agonist
31 responses. The [p.N855Sp.Asn855Ser](#) and [p.A172V-p.Ala172Val](#) variants increase activation
32 in response to agonists, although with distinct impacts on the biophysical properties of the
33 channel. Intrinsic differences due to the positions of the variants within the channel
34 ([p.N855Sp.Asn855Ser](#) is in the transmembrane domain S4), might underlie the differences
35 observed. Our data show that the ankyrin repeat domain is important in TRPA1 channel
36 activation and gating functions. The [p.A172V-p.Ala172Val](#) variant is reported at a
37 heterozygous frequency of 0.0003 in gnomAD and individuals over 70 years of age are
38 reportedly healthy so it is unlikely to be fully penetrant. It is more likely to act as a risk factor
39 and contribute to the expression of neuropathic pain by altering the functional properties of
40 nociceptive afferents; however, the drivers for channel activation (environmental versus
41 endogenous ligands) are not known.
42
43
44
45
46
47
48

49 In our study we identified clinically relevant variants in 12% of the participants, with impact
50 on clinical care and treatment. The majority of these variants [were are located](#) in ion channels
51 which are enriched in nociceptors and environmental triggers (such as cold in the case of non-
52 freezing cold injury) may interact and enhance the gain of function impact of such variants.
53
54
55
56
57
58
59
60

Acknowledgements:

Thank you to all the patients who took part in the study.

This research was funded in whole, or in part, by the Wellcome Trust (Grant numbers: 109915/Z/15/Z, 083259, 202747/Z/16/Z). For the purpose of open access, the author has applied a CC BY public copyright licence to any Author Accepted Manuscript version arising from this submission.

D.L.H.B., A.C.T, and A.S.C.R, are members of the DOLORisk consortium funded by the European Commission Horizon 2020 (ID633491), which received funding from European Union's Seventh Framework Program (FP7/2007-2013). D.L.H.B., and A.C.T are members of the International Diabetic Neuropathy Consortium (IDNC) research programme, which is supported by a Novo Nordisk Foundation Challenge Programme grant (Grant number NNF14OC0011633). D.L.H.B. is a Wellcome Investigator (202747/Z/16/Z and 223149/Z/21/Z). This work was supported by the Wellcome Trust through a Strategic Award to the London Pain Consortium (ref. no. 083259). D.L.H.B and A.C.T, are members of the PAINSTORM consortium funded by UKRI and Versus Arthritis. A.C.T is supported by Academy of Medical Sciences Starter Grant SGL022\1086, and is a Honorary Senior Research Fellow and Carnegie-Wits Diaspora Fellow at the Brain Function Research Group, School of Physiology, Faculty of Health Sciences, University of the Witwatersrand, Johannesburg, South Africa. R.H. is a Wellcome Trust Investigator (109915/Z/15/Z), who receives support from the Medical Research Council (UK) (MR/N025431/1 and MR/V009346/1), the European Research Council (309548), the Newton Fund (UK/Turkey, MR/N027302/1), the Addenbrookes Charitable Trust (G100142), the Evelyn Trust, the Stoneygate Trust, the Lily Foundation and an MRC strategic award to establish an International Centre for Genomic Medicine in Neuromuscular Diseases (ICGNMD) MR/S005021/1. M.M.R. acknowledges funding from the Medical Research Council (MRC MR/S005021/1), the National Institutes of Neurological Diseases and Stroke and office of Rare Diseases (U54NS065712 and 1UOINS109403-01 and R21TROO3034), Muscular Dystrophy Association (MDA510281) and the Charcot Marie Tooth Association (CMTA). This research was supported by the NIHR Cambridge Biomedical Research Centre (BRC-1215-20014). The views expressed are those of the authors and not necessarily those of the NIHR or the Department of Health and Social Care.

Authorship contributions:

- 1) conception and design of the study – ACT, GB, IB, MC, KM, DLHB
- 2) acquisition and analysis of data - all authors
- 3) drafting a significant portion of the manuscript or figures – ACT, GB, IB, MC, KM, DLHB

Conflict of Interest/Disclosures:

D.L.H.B. has acted as a consultant on behalf of Oxford Innovation for Amgen, Bristows, LatigoBio, GSK, Ionis, Lilly, Olipass, Orion, Regeneron and Theranexus on behalf of Oxford University Innovation over the last 2 years. He has received research funding from Lilly. He has received an industrial partnership grant from the BBSRC and AstraZeneca.

ASCR declares the following interests occurring in last 24 months: undertakes consultancy and advisory board work for Imperial College Consultants that included remunerated work for: Abide, Confo, Vertex, Pharmanovo, Lateral, Novartis, Mundipharma, Orion, Shanghai SIMR BiotechAsahi Kasei, Toray & Theranexis; owner of share options in Spinifex Pharmaceuticals from which personal benefit accrued upon the acquisition of Spinifex by Novartis in July 2015 (final payment was made in 2019); named as an inventor on patents: Rice A.S.C., Vandevoorde S. and Lambert D.M Methods using N-(2-propenyl)hexadecanamide and related amides to relieve pain. WO 2005/079771 and Okuse K. et al Methods of treating pain by inhibition of vgf activity EP13702262.0/ WO2013 110945; Member Joint Committee on Vaccine and Immunisation- varicella sub-committee; Analgesic Clinical Trial Translation: Innovations, Opportunities, and Networks (ACTION) steering committee member; Medicines and Healthcare products Regulatory Agency (MHRA), Commission on Human Medicines - Neurology, Pain & Psychiatry Expert Advisory Group

Figure and Table legends

Figure 1

Flow diagram outlining neuropathic pain grading, study participant recruitment and summary of study participant clinical phenotype

Ten participants were excluded due to either samples not received, quality control failures or gender discrepancies.

□ - Included cases of longstanding progressive neuropathies where the presenting or predominant feature was altered sensory function and an underlying cause could not be identified

¶ - Include cases of post herpetic neuralgia, episodic pain syndromes, neuropathic pain with plausible neuroanatomical distribution but no abnormalities on examination and specialised tests, leprosy, hereditary neuralgic amyotrophy, type 1 complex regional pain syndrome, Noonan syndrome, injury to left arm (these cases were included due to severe pain which was in excess of the inciting injury).

* - Genes selected for electrophysiological characterisation

NOS- Not otherwise specified

Figure 2

a) p.R185Hp.Arg185His is more common in non-freezing cold injury than control populations.

b) Schematic of $\text{Na}_v1.7$ channel topology. R185H is represented with a red dot.

c) Normalized peak current-voltage relationship curves for the WT at 20°C (black squares, $V_{1/2} = -30.7 \pm 1.3$, $k = 4.9 \pm 0.4$, $n=15$), WT at 10°C (grey dots, $V_{1/2} = -26.5 \pm 2$, $k = 6.6 \pm 0.6$, $n=14$), R185H at 20°C (red triangles, $V_{1/2} = -31.7 \pm 1.7$, $k = 5 \pm 0.5$, $n=15$), R185H at 10°C (blue diamonds, $V_{1/2} = -23.8 \pm 1.8$, $k = 6.7 \pm 0.5$, $n=13$). R185H was not significantly different when compared to WT ($p > 0.05$, Two-way ANOVA with Sidak's multiple comparison test, temperature and genotype are categorical variables). Currents elicited from a holding potential of -100 mV to different test pulse potentials (50ms) ranging from -80 to 40mV in 5mV increments. A holding potential of -100mV and an intersweep interval of 10s was used for all the protocols.

d) Steady-state fast inactivation curves for the WT at 20°C (black squares, $V_{1/2} = -85.8 \pm 1.8$, $k = 7.5 \pm 0.6$, $n=14$), WT at 10°C (grey dots, $V_{1/2} = -80 \pm 1.8$, $k = 13.7 \pm 0.6$, $n=13$), R185H at 20°C (red triangles, $V_{1/2} = -86.9 \pm 1.5$, $k = 7.6 \pm 0.3$, $n=14$), R185H at 10°C (blue diamonds, $V_{1/2} = -73.1 \pm 2.4$, $k = 14.7 \pm 0.6$, $n=13$). R185H significantly different when compared to WT at 10°C ($p < 0.05$, Two-way ANOVA with Sidak's multiple comparison test, temperature and genotype are categorical variables). Currents elicited with test pulses to -10 mV following 500 ms inactivating prepulses.

e) Open-state fast-inactivation kinetics for the WT at 20°C (black squares, $n=15$), WT at 10°C (grey dots, $n=14$), R185H at 20°C (red triangles, $n=15$), R185H at 10°C (blue diamonds, $n=13$).

f) Normalized peak current-voltage relationship curves for the WT at 20°C (black squares, $V_{1/2} = -30.7 \pm 1.3$, $k = 4.9 \pm 0.4$, $n=15$), WT at 30°C (light blue stars, $V_{1/2} = -34 \pm 1$, $k = 5.2 \pm 2.8$, $n=12$), R185H at 20°C (red triangles, $V_{1/2} = -31.7 \pm 1.7$, $k = 5 \pm 0.5$, $n=15$), R185H at 30°C (pink asterisks, $V_{1/2} = -33.6 \pm 2$, $k = 4.8 \pm 0.5$, $n=10$). Currents elicited from a holding potential

of -100 mV to different test pulse potentials (50ms) ranging from -80 to 40mV in 5mV increments

g) Steady-state fast inactivation curves for the WT at 20°C (black squares, $V_{1/2} = -85.8 \pm 1.8$, $k = 7.5 \pm 0.6$, $n=14$), WT at 30°C (light blue stars, $V_{1/2} = -86.3 \pm 2.1$, $k = 7.5 \pm 0.3$, $n=12$), R185H at 20°C (red triangles, $V_{1/2} = -86.9 \pm 1.5$, $k = 7.6 \pm 0.3$, $n=14$), R185H at 30°C (pink asterisks, $V_{1/2} = -85.9 \pm 2.4$, $k = 9 \pm 1.5$, $n=9$). Currents elicited with test pulses to -10 mV following 500 ms inactivating prepulses.

h) Open-state fast-inactivation kinetics for WT at 20°C (black squares, $n=15$), WT at 30°C (light blue stars, $n=12$), p.R185Hp.Arg185His at 20°C (red triangles, $n=15$), R185H at 30°C (pink asterisks, $n=10$).

NFCI – Non-freezing cold injury

NPD – Neuropathic Pain Disorders

WT – Wild Type

Data are presented as mean \pm SEM.

Statistical analysis for group comparisons - Two-way ANOVA with Sidak's multiple comparison test (*-statistically significant differences, $P < 0.05$)

Figure 3

a) p.A172V-p.Ala172Val variant: Alanine is substituted with a valine in the 4th ankyrin repeat domain of the channel. The residue is moderately conserved across different mammalian species.

b) Schematic of TRPA1 channel topology. p.A172Vp.Ala172Val variant is represented with a blue dot.

Voltage-dependence activation of hTRPA1 p.A172V-p.Ala172Val and p.N855Sp.Asn855Ser was measured in response to AITC. Current-voltage curves were measured with a two voltage-step protocol (voltage-ramps ranging from -100 mV to +100 mV for 500 ms, every 5 seconds). Holding potential was set at -70 mV. Application of 25 μ M of AITC shows enhanced activity of p.A172V p.Ala172Val variant in response to 25 μ M AITC in the presence of extracellular calcium alone (c-g).

c) Current density, assessed using a two-voltage step protocol, was significantly different between WT and variant channels as quantified in d) and e)

d) Outward currents (+100mV, WT= 21.12 ± 2.46 pA/pF, p.A172Vp.Arg185His= 56.92 ± 12.52 pA/pF, p.N855Sp.Asn855Ser = 38.12 ± 10.77 pA/pF) were significantly increased for p.A172V-p.Ala172Val ($p < 0.005$)

e) Inward currents (-100mV, WT= -6.12 ± 0.63 pA/pF, p.A172Vp.Arg185His= -8.48 ± 1.37 pA/pF, p.N855Sp.Asn855Ser = -13.48 ± 2.40 pA/pF) were significantly increased for p.N885S ($p < 0.005$)

f) Tail current analysis showed a significant shift in half-maximal activation potential for both p.A172V-p.Ala172Val ($n = 9$, $V_{1/2} = 35.55 \pm 5.45$ mV, and p.N855Sp.Asn855Ser, $V_{1/2} = 37.03 \pm 8.28$ mV $n = 12$, when compared to WT $n = 13$, $V_{1/2} = 59.16 \pm 5.25$ mV; $p < 0.05$). Slopes of the voltage-activation curve (i.e. voltage sensitivity) ($k = 49.38 \pm 2.03$ mV WT, $k = 43.29 \pm 2.63$ mV A172V, $k = 45.20 \pm 2.36$ mV; $p = 0.18$) were not significantly different.

g) Current-voltage relationships were tested with a voltage-ramp protocol in which voltage changes at a steady rate and the resulting current is recorded. After administration of 25 μ M (arrow) averaged currents from voltage-ramps were extrapolated and at +90mV showed a three-fold increase in current densities at positive potentials after application of 25 μ M AITC (WT = 85.13 \pm 23.30mV, p.A172V-p.Ala172Val = 250.4 \pm 62.39mV, p.N855Sp.Asn855Ser = 256.1 \pm 54.90mV; p<0.05). Insert shows example tracing.

WT – Wild Type

Data are presented as mean \pm SEM.

Statistical analysis for group comparisons - One way ANOVA with Sidak's multiple comparison test (* - indicates statistically significant differences, P <0.05)

Figure 4:

Application of 100 μ M of Menthol in the presence of intracellular and extracellular calcium shows enhanced activity of p.A172V-p.Ala172Val and p.N855Sp.Asn855Ser variants. Current-voltage curves were measured with a two voltage-step protocol (voltage-ramps ranging from -100 mV to + 100 mV for 500 ms, every 5 seconds; holding potential was set at -70 mV).

a) Current density, assessed using a two-voltage step protocol, in WT and variant channels were significantly different as quantified in d) and e)

b) Outward currents were enhanced for both p.A172V-p.Ala172Val and p.N855Sp.Asn855Ser (+100mV, WT = 21.96 \pm 3.64mV, p.Ala172Val = 39.94 \pm 5.80mV, and p.N855Sp.Asn855Ser = 70.07 \pm 21.71mV; p<0.05)

c) Inward currents were not statistically different (-100mV, WT = -8.29 \pm 1.97mV, -6.52 \pm 0.83mV p.Ala172Val, and p.N855Sp.Asn855Ser = -5.72 \pm 0.94mV; p = 0.58, and p = 0.40, respectively)

d) Half-maximal activation potential was significantly shifted leftward for p.A172V-p.Ala172Val and p.N855Sp.Asn855Ser (V_{1/2}, WT= 61.83 \pm 7.37mV n = 8, p.A172V-p.Ala172Val = 36.41 \pm 7.58mV n = 9, p.N855Sp.Asn855Ser = 33.60 \pm 6.67mV n = 6). Voltage sensitivity was significantly altered (slope factor k = 41.51 \pm 2.33mV WT; 40.21 \pm 2.98mV p.A172V-p.Arg185His; 39.32 \pm 3.03mV p.N855Sp.Asn855Ser; p<0.05).

WT – Wild Type

Data are presented as mean \pm SEM.

Statistical analysis for group comparisons - One way ANOVA with Sidak's multiple comparison test (* - indicates statistically significant differences, P <0.05)

Table 1

A summary of the neuropathic pain disorders and the key diagnostic criteria used to classify the study participants enrolled. Pattern of inheritance for the Mendelian inherited pain disorders, genes (including the OMIM reference), and important PMID references and are listed.

NOS- Not otherwise specified

NPD- Neuropathic pain disorder.

Table 2

A summary of the genes shown to have a causal role in neuropathic pain and included in our analysis. At the time of recruitment, 2015, a list of 14 genes with an established causal role in neuropathic pain was curated (Tier 1 genes). The criteria for a gene inclusion were at least three independent families reported with a causal variant in the gene, or two families with additional in vitro functional studies and/or mouse model (Turro *et al.*, 2020).

If genes were implicated in neuropathic pain, but did not meet Tier 1 criteria, they were classified as Tier 2 genes. Genes of interest, as determined by expert consensus with little or no published data, were classified as Tier 3 genes. Before exploratory analysis of Tier 2 and 3 genes a contemporaneous search was performed to identify new genes that had been described in the ensuing period from the start of the project to the analysis of data (2015-2021). These genes were included in the tier 2 and 3 gene analysis

HSAN - Hereditary and Autonomic Sensory Neuropathy

HGNC - HUGO Gene Nomenclature Committee:

Table 3

List of gene variants that were reported ~~that~~ and were deemed medically actionable i.e. variants that result in specific, defined medical recommendations. Clinically relevant, medically actionable, variants were reported to the referring clinician.

All participants were heterozygous for the relevant variants

All variants were predicted by Ensembl Variant Effect Predictor as missense variants

VUS – variant of uncertain significance

gnomAD - Genome Aggregation Database, open resource that aggregates and harmonises both exome and genome sequencing data; current status lists 125,748 exome sequences and 15,708 whole-genome sequences from unrelated individuals sequenced as part of various disease-specific and population genetic studies.

Allele Frequencies are shown in the Neuropathic Pain Disorders (NPD) cohort and in NIHR BioResource control cohorts.

WGS10K – NIHR Bioresources database with 13,037 whole genome sequences.

NPD- Neuropathic Pain Disorders

In silico analysis, SIFT and Polyphen, results shown.

1
2
3 SIFT score predicts whether an amino acid substitution affects protein function. The SIFT score
4 ranges from 0.0 (deleterious) to 1.0 (tolerated).

5
6 The score can be interpreted as follows:

7 0.0 to 0.05 - Variants with scores in this range are considered deleterious. Variants with scores
8 closer to 0.0 are more confidently predicted to be deleterious.

9
10 0.05 to 1.0 - Variants with scores in this range are predicted to be tolerated (benign). Variants
11 with scores very close to 1.0 are more confidently predicted to be tolerated.

12 13 14 **Table 4**

15 Results from the gene-wise association test (using the gene-wise approach of the combined
16 burden and variance-component test SKAT-O) for rare variants of Tier 1-3 genes and
17 functionally validated variants of the *SCN9A*, *SCN10A*, *SCN11A* genes for all participants with
18 neuropathic pain.

19 Significance was set to the Bonferroni adjusted 0.01 threshold for the number of genes
20 considered ($0.01/36 = 2.7 \times 10^{-4}$). We report unadjusted P values that passed the Bonferroni
21 corrected significant threshold.

22
23
24
25
26 The genomic coordinates and the HGNC gene symbol of the gene models that have a
27 significantly different configuration of rare variants between cases and controls are presented
28 in the first column. The second column holds the fraction of individuals carrying rare variants
29 below the MAF threshold < 0.05 . We show the number of variants considered for the
30 association, followed by the P value of the association test. The last column holds the Rho
31 statistic.

32
33 Values can be interpreted as:

34 Rho = 0, causal and non-causal variants with opposing directions driving the association to
35 Rho=1, high percentage of causal variants acting in the same direction driving the association.
36 Results are grouped by ethnicity and phenotype.

37 38 39 40 41 **Supplementary table 1**

42 Significant results from the gene-wise association test for rare variants of Tier 1-3 genes for
43 each ethnicity and phenotype. Significance was set to the Bonferroni adjusted 0.01 threshold
44 for the number of genes considered ($0.01/36 = 2.7 \times 10^{-4}$). We report unadjusted P values that
45 passed the Bonferroni corrected significant threshold.

46 47 48 49 **Supplementary table 2**

50 Significant results from the gene-wise association test for the whole gene set (5790). For the
51 whole gene set analysis we applied a minor allele count filter of ≥ 2 and for the Neuropathic
52 Pain Disorders candidate genes a minor allele count filter of ≥ 1 . Only genes with at least two
53 variants which passed the filters were included.

54 Significance was set to the Bonferroni adjusted 0.01 threshold for the number of genes
55 considered ($0.01/5790 = 1.7 \times 10^{-6}$).

56
57
58
59
60 .

Supplementary figures and legends

Supplementary figure 1

Flow diagram outlining recruitment of participants, analysis pipeline and genetic testing and the difference between the clinical reporting of relevant gene variants versus the exploratory gene analysis and in vitro functional assessment of variants of interest

Supplementary figure 2

Flow diagram outlining neuropathic pain grading .

Possible neuropathic pain must fulfil criteria 1 and 2.

33tp3 Probable neuropathic pain must fulfil criteria 1, 2 and 3.

Definite neuropathic pain must fulfil all 4 criteria.

1. Pain with a distinct neuroanatomically plausible distribution e.g. pain symmetrically distributed in the extremities, pain in erythematous areas
2. A history suggestive of a relevant lesion or disease affecting the peripheral or central somatosensory system e.g. a history of neuropathy symptoms including decreased sensation, or positive sensory symptoms e.g. burning, aching pain mainly in the toes, feet or legs.
3. Demonstration of distinct neuroanatomically plausible distribution of neuropathic pain e.g. presence of clinical signs of peripheral neuropathy such as decreased distal sensation or decreased/absent ankle reflexes.
4. Demonstration of the relevant lesion or disease by at least one confirmatory test e.g. abnormality on either nerve conduction tests, thermal thresholds or intra-epidermal nerve fibre density.

Supplementary figure 3

Biophysical characterisation of hTRPA1 WT, ~~p.A172V~~ p.Ala172Val and p.N855Sp.Asn855Ser variant in control conditions shows no significant differences. Voltage step protocol consisted of 400 ms voltage steps to test potentials ranging from -100 mV to +180 mV, followed by a final invariant step to -75 mV (400 ms to measure tail currents). The holding potential was set at -0 mV.

a) Current density measured in WT and mutant channels were not statistically different as quantified in b) and c)

b) Outward currents at (+100mV, WT = 15.41 ± 3.01 pA/pF, ~~p.A172V~~ p.Ala172Val = 16.69 ± 2.85 pA/pF, p. AsNn855Ser = 23.81 ± 4.25 pA/pF) were not significantly different between WT and the respective variants (p = 0.77 WT versus p.Ala172+V2al, p = 0.17 WT versus p.AsNn855Ser)

c) Inward currents (at -100mV, WT = -5.42 ± 0.68 pA/pF, p.Ala172Val = -6.80 ± 1.18 pA/pF and N855Sp.Asn855Ser = -10.66 ± 3.00 pA/pF), were not significantly different between WT and the respective variants (p = 0.75 WT versus p.Ala172+Val2, and p = 0.05 WT versus N855Sp.Asn855Ser).

d) Voltage of half-maximal activation for WT n = 12, ~~p.A172V~~ p.Ala172Val n = 9 and p.N855Sp.Asn855Ser n = 7 ($V_{1/2}$, WT = 59.70 ± 4.59 mV, ~~p.A172V~~ p.Ala172Val = $59.45 \pm$

8.91mV, [p.N855Sp.Asn855Ser](#) = 64.85 ± 8.09mV; p= 0.99, and p = 0.85, respectively) and slopes of the voltage-activation curve (k, WT = 42.51 ± 2.01mV, [p.A172V-p.Ala172Val](#) = 46.19 ± 2.60mV, [p.N855Sp.Asn855Ser](#) = 47.45 ± 1.88mV; p = 0.41 and p = 0.26, respectively) were not statistically different.

WT – Wild Type

Data are presented as mean ± SEM.

Statistical analysis for group comparisons - One way ANOVA with Sidak's multiple comparison test (* - indicates statistically significant differences, P <0.05)

Supplementary figure 4:

Application of 100µM of Menthol, with extracellular calcium alone, did not alter [p.A172V-p.Ala172Val](#) nor [p.N855Sp.Asn855Ser](#) channel excitability. Voltage-dependence activation of hTRPA1 [p.A172V-p.Ala172Val](#) and [p.N855Sp.Asn855Ser](#) was measured in response to Menthol. Current-voltage curves were measured with a two voltage-step protocol (voltage-ramps ranging from -100 mV to + 100 mV for 500 ms, every 5 seconds; holding potential was set at -70 mV).

a) Current densities were not statistically different for the variant channels when compared to WT as quantified in b) and c)

b) Outward current (at +100mV, WT = 13.29 ± 1.69pA/pF, [p.A172V-p.Ala172Val](#) = 17.51 ± 2.60pA/pF, [p.N855Sp.Asn855Ser](#) = 20.66 ± 3.35pA/pF were not significantly different (p = 0.44, and p = 0.15, respectively).

c) Inward currents (at -100mV, WT = -6.02 ± 1.11pA/pF, [p.A172V-p.Ala172Val](#) = -7.66 ± 1.83pA/pF, [p.N855Sp.Asn855Ser](#) = -7.49 ± 1.53pA/pF) were not significantly different (p = 0.72, p = 0.80, respectively).

d) Half-maximal activation voltage for WT n = 8, [p.A172V-p.Ala172Val](#) n = 8, and [N855Sp.Asn855Ser](#) n = 7 ($V_{1/2}$, WT= 65.39 ± 5.79mV, [p.A172Vp.Arg185His](#)= 56.61 ± 9.25mV, [p.Asn855Serp.N855Sp.Asn855Ser](#)= 58.62 ± 7.31mV, p = 0.69, and p = 0.83, respectively) were not statistically different. Slopes of the voltage-activation curve (k = 56.66 ± 1.40mV WT, 49.01 ± 1.53mV [p.A172Vp.Arg185His](#), 49.73 ± 3.28mV [N855Sp.Asn855Ser](#), p= 0.022 and p = 0.069, respectively) were reduced for both [p.A172V](#) and [p.N855Sp.Asn855Ser](#).

WT – Wild Type

Data are presented as mean ± SEM.

Statistical analysis for group comparisons - One way ANOVA with Sidak's multiple comparison test (* - indicates statistically significant differences, P <0.05).

References:

Alsouloum M, Higerd GP, Effraim PR, Waxman SG. Status of peripheral sodium channel blockers for non-addictive pain treatment. *Nat Rev Neurol* 2020; 16(12): 689-705.

Attal N, Lanteri-Minet M, Laurent B, Fermanian J, Bouhassira D. The specific disease burden of neuropathic pain: results of a French nationwide survey. *Pain* 2011; 152(12): 2836-43.

Avenali L, Narayanan P, Rouwette T, Cervellini I, Sereda M, Gomez-Varela D, *et al.* Annexin A2 Regulates TRPA1-Dependent Nociception. *The Journal of Neuroscience* 2014a; 34(44): 14506-16.

Avenali L, Narayanan P, Rouwette T, Cervellini I, Sereda M, Gomez-Varela D, *et al.* Annexin A2 regulates TRPA1-dependent nociception. *J Neurosci* 2014b; 34(44): 14506-16.

Benedsgaard K, Ventzel L, Grafe P, Tigerholm J, Themistocleous AC, Bennett DL, *et al.* Cold aggravates abnormal excitability of motor axons in oxaliplatin-treated patients. *Muscle & Nerve* 2020; 61(6): 796-800.

Bennett DL, Clark AJ, Huang J, Waxman SG, Dib-Hajj SD. The Role of Voltage-Gated Sodium Channels in Pain Signaling. *Physiol Rev* 2019; 99(2): 1079-151.

Bennett DL, Woods CG. Painful and painless channelopathies. *Lancet Neurol* 2014; 13(6): 587-99.

Blesneac I, Themistocleous AC, Fratter C, Conrad LJ, Ramirez JD, Cox JJ, *et al.* Rare NaV1.7 variants associated with painful diabetic peripheral neuropathy. *PAIN* 2018; 159(3): 469-80.

Bouhassira D, Attal N, Alchaar H, Boureau F, Brochet B, Bruxelle J, *et al.* Comparison of pain syndromes associated with nervous or somatic lesions and development of a new neuropathic pain diagnostic questionnaire (DN4). *PAIN* 2005; 114(1-2): 29-36.

Calvo M, Davies AJ, Hébert HL, Weir GA, Chesler EJ, Finnerup NB, *et al.* The Genetics of Neuropathic Pain from Model Organisms to Clinical Application. *Neuron* 2019; 104(4): 637-53.

Carroll A, Dyck PJ, de Carvalho M, Kennerson M, Reilly MM, Kiernan MC, *et al.* Novel approaches to diagnosis and management of hereditary transthyretin amyloidosis. *J Neurol Neurosurg Psychiatry* 2022; 93(6): 668-78.

Cox JJ, Reimann F, Nicholas AK, Thornton G, Roberts E, Springell K, *et al.* An SCN9A channelopathy causes congenital inability to experience pain. *Nature* 2006; 444(7121): 894-8.

1
2
3 Cregg R, Cox JJ, Bennett DLH, Wood JN, Werdehausen R. Mexiletine as a treatment for
4 primary erythromelalgia: normalization of biophysical properties of mutant L858F Nav1.7
5 sodium channels. *Br J Pharmacol* 2014; 171(19): 4455-63.
6
7

8 Cummins TR, Dib-Hajj SD, Waxman SG. Electrophysiological properties of mutant Nav1.7
9 sodium channels in a painful inherited neuropathy. *J Neurosci* 2004; 24(38): 8232-6.
10
11

12 Davidson GL, Murphy SM, Polke JM, Laura M, Salih MAM, Muntoni F, *et al.* Frequency of
13 mutations in the genes associated with hereditary sensory and autonomic neuropathy in a UK
14 cohort. *Journal of neurology* 2012; 259(8): 1673-85.
15
16

17 de Greef BTA, Hoeijmakers JGJ, Geerts M, Oakes M, Church TJE, Waxman SG, *et al.*
18 Lacosamide in patients with Nav1.7 mutations-related small fibre neuropathy: a randomized
19 controlled trial. *Brain* 2019; 142(2): 263-75.
20
21

22 Devigili G, Rinaldo S, Lombardi R, Cazzato D, Marchi M, Salvi E, *et al.* Diagnostic criteria
23 for small fibre neuropathy in clinical practice and research. *Brain* 2019; 142(12): 3728-36.
24
25

26 England JD, Gronseth GS, Franklin G, Miller RG, Asbury AK, Carter GT, *et al.* Distal
27 symmetric polyneuropathy: a definition for clinical research: report of the American Academy
28 of Neurology, the American Association of Electrodiagnostic Medicine, and the American
29 Academy of Physical Medicine and Rehabilitation. *Neurology* 2005; 64(2): 199-207.
30
31

32 Estacion M, Vohra BPS, Liu S, Hoeijmakers J, Faber CG, Merkies ISJ, *et al.* Ca²⁺ toxicity
33 due to reverse Na⁺/Ca²⁺ exchange contributes to degeneration of neurites of DRG neurons
34 induced by a neuropathy-associated Nav1.7 mutation. *Journal of Neurophysiology* 2015;
35 114(3): 1554-64.
36
37

38 Faber CG, Hoeijmakers JGJ, Ahn H-S, Cheng X, Han C, Choi J-S, *et al.* Gain of function
39 Nav1.7 mutations in idiopathic small fiber neuropathy. *Annals of Neurology* 2012a; 71(1): 26-
40 39.
41
42

43 Faber CG, Lauria G, Merkies IS, Cheng X, Han C, Ahn HS, *et al.* Gain-of-function Nav1.8
44 mutations in painful neuropathy. *Proc Natl Acad Sci U S A* 2012b; 109(47): 19444-9.
45
46

47 Fertleman CR, Baker MD, Parker KA, Moffatt S, Elmslie FV, Abrahamsen B, *et al.* SCN9A
48 mutations in paroxysmal extreme pain disorder: allelic variants underlie distinct channel
49 defects and phenotypes. *Neuron* 2006; 52(5): 767-74.
50
51

52 Finnerup NB, Attal N, Haroutounian S, McNicol E, Baron R, Dworkin RH, *et al.*
53 Pharmacotherapy for neuropathic pain in adults: a systematic review and meta-analysis. *The*
54 *Lancet Neurology* 2015; 14(2): 162-73.
55
56
57
58
59
60

1
2
3 Finnerup NB, Haroutounian S, Kamerman P, Baron R, Bennett DLH, Bouhassira D, *et al.*
4 Neuropathic pain: an updated grading system for research and clinical practice. *PAIN* 2016;
5 157(8): 1599-606.
6
7

8
9 Geha P, Yang Y, Estacion M, Schulman BR, Tokuno H, Apkarian AV, *et al.* Pharmacotherapy
10 for Pain in a Family With Inherited Erythromelalgia Guided by Genomic Analysis and
11 Functional Profiling. *JAMA Neurol* 2016; 73(6): 659-67.
12

13
14 Han C, Hoeijmakers JGJ, Liu S, Gerrits MM, te Morsche RHM, Lauria G, *et al.* Functional
15 profiles of SCN9A variants in dorsal root ganglion neurons and superior cervical ganglion
16 neurons correlate with autonomic symptoms in small fibre neuropathy. *Brain* 2012; 135(9):
17 2613-28.
18

19
20 Han C, Lampert A, Rush AM, Dib-Hajj SD, Wang X, Yang Y, *et al.* Temperature Dependence
21 of Erythromelalgia Mutation L858F in Sodium Channel Nav1.7. *Molecular Pain* 2007; 3: 1744-
22 8069-3-3.
23

24
25 Han C, Vasylyev D, Macala LJ, Gerrits MM, Hoeijmakers JG, Bekelaar KJ, *et al.* The G1662S
26 NaV1.8 mutation in small fibre neuropathy: impaired inactivation underlying DRG neuron
27 hyperexcitability. *J Neurol Neurosurg Psychiatry* 2014; 85(5): 499-505.
28

29
30 Hébert HL, Veluchamy A, Torrance N, Smith BH. Risk factors for neuropathic pain in diabetes
31 mellitus. *Pain* 2017; 158(4): 560-8.
32

33
34 Heyne HO, Baez-Nieto D, Iqbal S, Palmer DS, Brunklaus A, May P, *et al.* Predicting functional
35 effects of missense variants in voltage-gated sodium and calcium channels. *Sci Transl Med*
36 2020; 12(556).
37

38
39 Hoeijmakers JGJ, Han C, Merkies ISJ, Macala LJ, Lauria G, Gerrits MM, *et al.* Small nerve
40 fibres, small hands and small feet: a new syndrome of pain, dysautonomia and acromesomelia
41 in a kindred with a novel NaV1.7 mutation. *Brain* 2012; 135(2): 345-58.
42
43

44
45 Kleyweg RP, van der Meché FG, Schmitz PI. Interobserver agreement in the assessment of
46 muscle strength and functional abilities in Guillain-Barré syndrome. *Muscle Nerve* 1991;
47 14(11): 1103-9.
48

49
50 Kremeyer B, Lopera F, Cox JJ, Momin A, Rugiero F, Marsh S, *et al.* A gain-of-function
51 mutation in TRPA1 causes familial episodic pain syndrome. *Neuron* 2010; 66(5): 671-80.
52

53
54 Labau JIR, Estacion M, Tanaka BS, de Greef BTA, Hoeijmakers JGJ, Geerts M, *et al.*
55 Differential effect of lacosamide on Nav1.7 variants from responsive and non-responsive
56 patients with small fibre neuropathy. *Brain* 2020; 143(3): 771-82.
57
58
59
60

1
2
3 Lauria G, Bakkers M, Schmitz C, Lombardi R, Penza P, Devigili G, *et al.* Intraepidermal nerve
4 fiber density at the distal leg: a worldwide normative reference study. *J Peripher Nerv Syst*
5 2010a; 15(3): 202-7.
6
7

8 Lauria G, Hsieh ST, Johansson O, Kennedy WR, Leger JM, Mellgren SI, *et al.* European
9 Federation of Neurological Societies/Peripheral Nerve Society Guideline on the use of skin
10 biopsy in the diagnosis of small fiber neuropathy. Report of a joint task force of the European
11 Federation of Neurological Societies and the Peripheral Nerve Society. *Eur J Neurol* 2010b;
12 17(7): 79-92.
13
14

15
16 Lee S, Emond MJ, Bamshad MJ, Barnes KC, Rieder MJ, Nickerson DA, *et al.* Optimal Unified
17 Approach for Rare-Variant Association Testing with Application to Small-Sample Case-
18 Control Whole-Exome Sequencing Studies. *The American Journal of Human Genetics* 2012a;
19 91(2): 224-37.
20
21

22 Lee S, Wu MC, Lin X. Optimal tests for rare variant effects in sequencing association studies.
23 *Biostatistics* 2012b; 13(4): 762-75.
24
25

26 Liu Y, Bian X, Wang K. Pharmacological Activation of Neuronal Voltage-Gated
27 Kv7/KCNQ/M-Channels for Potential Therapy of Epilepsy and Pain. *Handb Exp Pharmacol*
28 2021; 267: 231-51.
29
30

31 Macpherson LJ, Dubin AE, Evans MJ, Marr F, Schultz PG, Cravatt BF, *et al.* Noxious
32 compounds activate TRPA1 ion channels through covalent modification of cysteines. *Nature*
33 2007; 445(7127): 541-5.
34
35

36
37 Medical Research Council - Nerve Injuries Research Committee. Aids to the examination of
38 the peripheral nervous system. Fifth Edition ed: Saunders Elsevier on behalf of Guarantors of
39 Brain; 2010.
40
41

42 Noël J, Zimmermann K, Busserolles J, Deval E, Alloui A, Diochot S, *et al.* The mechano-
43 activated K⁺ channels TRAAK and TREK-1 control both warm and cold perception. *Embo j*
44 2009; 28(9): 1308-18.
45
46

47 Peters MJ, Bakkers M, Merkies IS, Hoeijmakers JG, van Raak EP, Faber CG. Incidence and
48 prevalence of small-fiber neuropathy: a survey in the Netherlands. *Neurology* 2013; 81(15):
49 1356-60.
50
51

52 Reimann F, Cox JJ, Belfer I, Diatchenko L, Zaykin DV, McHale DP, *et al.* Pain perception is
53 altered by a nucleotide polymorphism in SCN9A. *Proc Natl Acad Sci U S A* 2010; 107(11):
54 5148-53.
55
56

57 Richards S, Aziz N, Bale S, Bick D, Das S, Gastier-Foster J, *et al.* Standards and guidelines
58 for the interpretation of sequence variants: a joint consensus recommendation of the American
59
60

1
2
3 College of Medical Genetics and Genomics and the Association for Molecular Pathology.
4 Genet Med 2015; 17(5): 405-24.
5

6
7 Schon KR, Parker APJ, Woods CG. Congenital Insensitivity to Pain Overview. In: Adam MP,
8 Ardinger HH, Pagon RA, Wallace SE, Bean LJH, Stephens K, *et al.*, editors. GeneReviews(®).
9 Seattle (WA): University of Washington, Seattle; 1993.
10

11
12 Shnayder NA, Petrova MM, Popova TE, Davidova TK, Bobrova OP, Trefilova VV, *et al.*
13 Prospects for the Personalized Multimodal Therapy Approach to Pain Management via Action
14 on NO and NOS. Molecules 2021; 26(9).
15

16
17 The 100000 Genomes Project Pilot Investigators. 100,000 Genomes Pilot on Rare-Disease
18 Diagnosis in Health Care — Preliminary Report. New England Journal of Medicine 2021;
19 385(20): 1868-80.
20

21
22 Treede RD, Jensen TS, Campbell JN, Cruccu G, Dostrovsky JO, Griffin JW, *et al.* Neuropathic
23 pain: redefinition and a grading system for clinical and research purposes. Neurology 2008;
24 70(18): 1630-5.
25

26
27 Turro E, Astle WJ, Megy K, Gräf S, Greene D, Shamardina O, *et al.* Whole-genome sequencing
28 of patients with rare diseases in a national health system. Nature 2020; 583(7814): 96-102.
29

30
31 Vale TA, Symmonds M, Polydefkis M, Byrnes K, Rice ASC, Themistocleous AC, *et al.*
32 Chronic non-freezing cold injury results in neuropathic pain due to a sensory neuropathy. Brain
33 2017; 140(10): 2557-69.
34

35
36 van Hecke O, Austin SK, Khan RA, Smith BH, Torrance N. Neuropathic pain in the general
37 population: a systematic review of epidemiological studies. Pain 2014; 155(4): 654-62.
38

39
40 Yang Y, Dib-Hajj SD, Zhang J, Zhang Y, Tyrrell L, Estacion M, *et al.* Structural modelling
41 and mutant cycle analysis predict pharmacoresponsiveness of a Na(V)1.7 mutant channel. Nat
42 Commun 2012; 3: 1186.
43

44
45 Yang Y, Wang Y, Li S, Xu Z, Li H, Ma L, *et al.* Mutations in SCN9A, encoding a sodium
46 channel alpha subunit, in patients with primary erythralgia. J Med Genet 2004; 41(3): 171-
47 4.
48

49
50 Zhang Z, Schmelz M, Segerdahl M, Quiding H, Centerholt C, Juréus A, *et al.* Exonic mutations
51 in SCN9A (NaV1.7) are found in a minority of patients with erythromelalgia. Scand J Pain
52 2014; 5(4): 217-25.
53
54
55
56
57
58
59
60

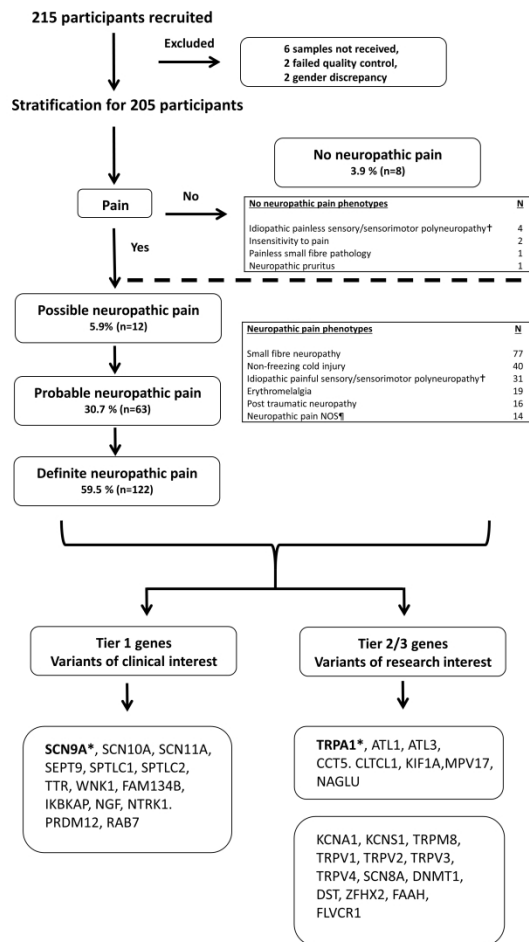


Figure 1

Figure 1

Flow diagram outlining neuropathic pain grading, study participant recruitment and summary of study participant clinical phenotype

Ten participants were excluded due to either samples not received, quality control failures or gender discrepancies.

□□ - Included cases of longstanding progressive neuropathies where the presenting or predominant feature was altered sensory function and an underlying cause could not be identified

¶ - Include cases of post herpetic neuralgia, episodic pain syndromes, neuropathic pain with plausible neuroanatomical distribution but no abnormalities on examination and specialised tests, leprosy, hereditary neuralgic amyotrophy, type 1 complex regional pain syndrome, Noonan syndrome, injury to left arm (these cases were included due to severe pain which was in excess of the inciting injury).

* - Genes selected for electrophysiological characterisation

NOS - Not otherwise specified

1
2
3
4
5
6
7
8
9
10
11
12
13
14
15
16
17
18
19
20
21
22
23
24
25
26
27
28
29
30
31
32
33
34
35
36
37
38
39
40
41
42
43
44
45
46
47
48
49
50
51
52
53
54
55
56
57
58
59
60

250x500mm (300 x 300 DPI)

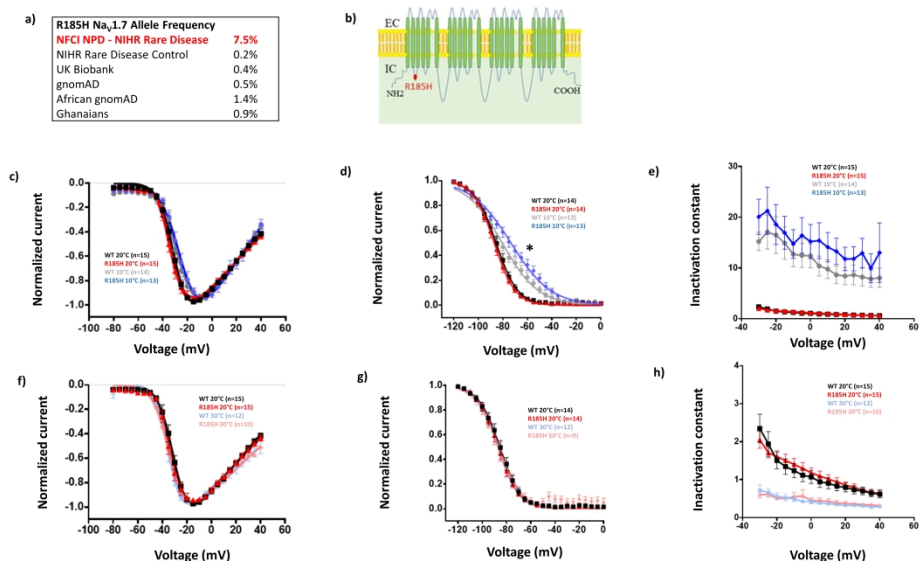


Figure 2

Figure 2

a) p.R185H is more common in non-freezing cold injury than control populations.

b) Schematic of NaV1.7 channel topology. R185H is represented with a red dot.

c) Normalized peak current-voltage relationship curves for the WT at 20°C (black squares, V_{1/2} = -30.7 ± 1.3, k = 4.9 ± 0.4, n=15), WT at 10°C (grey dots, V_{1/2} = -26.5 ± 2, k = 6.6 ± 0.6, n=14), R185H at 20°C (red triangles, V_{1/2} = -31.7 ± 1.7, k = 5 ± 0.5, n=15), R185H at 10°C (blue diamonds, V_{1/2} = -23.8 ± 1.8, k = 6.7 ± 0.5, n=13). R185H was not significantly different when compared to WT (p > 0.05).

Currents elicited from a holding potential of -100 mV to different test pulse potentials (50ms) ranging from -80 to 40mV in 5mV increments. A holding potential of -100mV and an intersweep interval of 10s was used for all the protocols.

d) Steady-state fast inactivation curves for the WT at 20°C (black squares, V_{1/2} = -85.8 ± 1.8, k = 7.5 ± 0.6, n=14), WT at 10°C (grey dots, V_{1/2} = -80 ± 1.8, k = 13.7 ± 0.6, n=13), R185H at 20°C (red triangles, V_{1/2} = -86.9 ± 1.5, k = 7.6 ± 0.3, n=14), R185H at 10°C (blue diamonds, V_{1/2} = -73.1 ± 2.4, k = 14.7 ± 0.6, n=13). R185H significantly different when compared to WT at 10°C (p < 0.05). Currents elicited with test pulses to -10 mV following 500 ms inactivating prepulses.

e) Open-state fast-inactivation kinetics for the WT at 20°C (black squares, n=15), WT at 10°C (grey dots, n=14), R185H at 20°C (red triangles, n=15), R185H at 10°C (blue diamonds, n=13).

f) Normalized peak current-voltage relationship curves for the WT at 20°C (black squares, V_{1/2} = -30.7 ± 1.3, k = 4.9 ± 0.4, n=15), WT at 30°C (light blue stars, V_{1/2} = -34 ± 1, k = 5.2 ± 2.8, n=12), R185H at 20°C (red triangles, V_{1/2} = -31.7 ± 1.7, k = 5 ± 0.5, n=15), R185H at 30°C (pink asterisks, V_{1/2} = -33.6 ± 2, k = 4.8 ± 0.5, n=10). Currents elicited from a holding potential of -100 mV to different test pulse potentials (50ms) ranging from -80 to 40mV in 5mV increments.

g) Steady-state fast inactivation curves for the WT at 20°C (black squares, V_{1/2} = -85.8 ± 1.8, k = 7.5 ± 0.6, n=14), WT at 30°C (light blue stars, V_{1/2} = -86.3 ± 2.1, k = 7.5 ± 0.3, n=12), R185H at 20°C (red triangles, V_{1/2} = -86.9 ± 1.5, k = 7.6 ± 0.3, n=14), R185H at 30°C (pink asterisks, V_{1/2} = -85.9 ± 2.4, k = 9 ± 1.5, n=9). Currents elicited with test pulses to -10 mV following 500 ms inactivating prepulses.

h) Open-state fast-inactivation kinetics for WT at 20°C (black squares, n=15), WT at 30°C (light blue stars, n=12), p.R185H at 20°C (red triangles, n=15), R185H at 30°C (pink asterisks, n=10).

Data are presented as mean ± SEM.

Statistical analysis for group comparisons - Two-way ANOVA with Sidak's multiple comparison test, temperature and genotype are categorical variables (*-statistically significant differences, P < 0.05)

399x250mm (300 x 300 DPI)

1
2
3
4
5
6
7
8
9
10
11
12
13
14
15
16
17
18
19
20
21
22
23
24
25
26
27
28
29
30
31
32
33
34
35
36
37
38
39
40
41
42
43
44
45
46
47
48
49
50
51
52
53
54
55
56
57
58
59
60

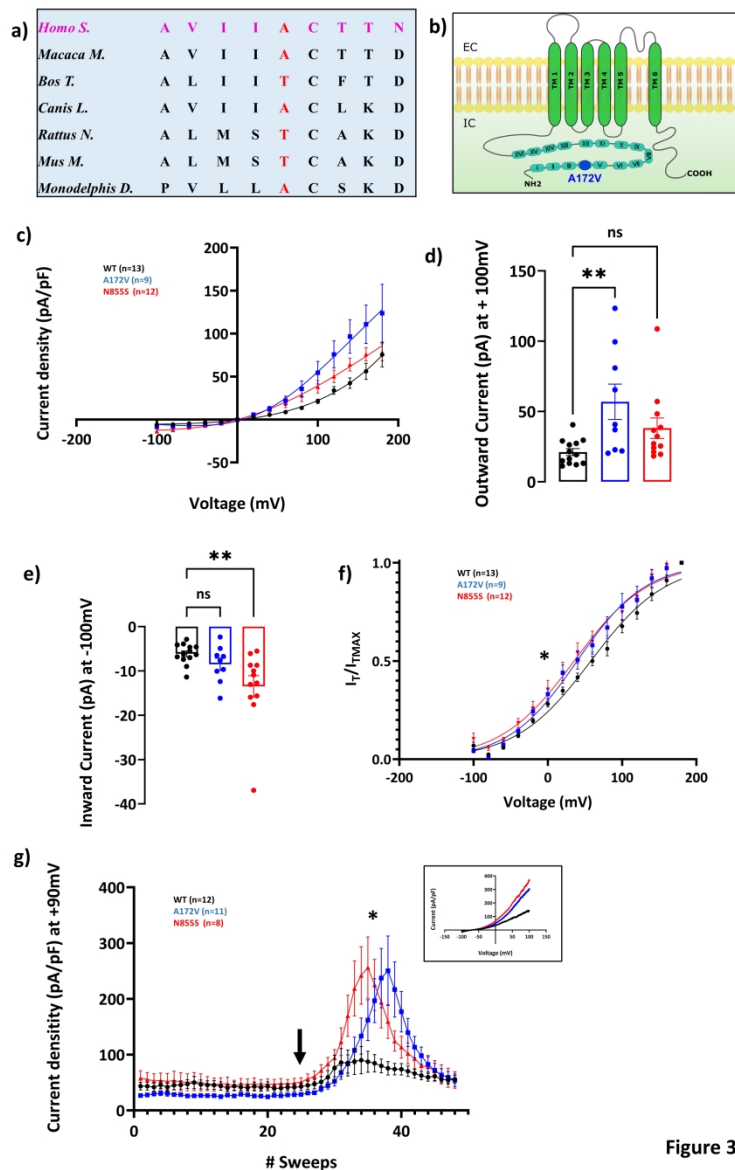


Figure 3

Figure 3

a) p.A172V variant: Alanine is substituted with a valine in the 4th ankyrin repeat domain of the channel. The residue is moderately conserved across different mammalian species.

b) Schematic of TRPA1 channel topology. p.A172V variant is represented with a blue dot.

Voltage-dependence activation of hTRPA1 p.A172V and p.N855S was measured in response to AITC. Current-voltage curves were measured with a two voltage-step protocol (voltage-ramps ranging from -100 mV to +100 mV for 500 ms, every 5 seconds). Holding potential was set at -70 mV. Application of 25 μ M AITC shows enhanced activity of p.A172V variant in response to 25 μ M AITC in the presence of extracellular calcium alone (c-g).

c) Current density, assessed using a two-voltage step protocol, was significantly different between WT and variant channels as quantified in d) and e)

d) Outward currents (+100mV, WT = 21.12 ± 2.46 pA/pF, p.A172V = 56.92 ± 12.52 pA/pF, p.N855S = 38.12 ± 10.77 pA/pF) were significantly increased for p.A172V ($p < 0.005$)

1
2
3 e) Inward currents (-100mV, WT= -6.12 ± 0.63 pA/pF, p.A172V= -8.48 ± 1.37 pA/pF, p.N855S = $-13.48 \pm$
4 2.40 pA/pF) were significantly increased for p.N885S ($p < 0.005$)

5 f) Tail current analysis showed a significant shift in half-maximal activation potential for both p.A172V ($n =$
6 9 , $V_{1/2} = 35.55 \pm 5.45$ mV, and p.N855S, $V_{1/2} = 37.03 \pm 8.28$ mV $n = 12$, when compared to WT $n = 13$,
7 $V_{1/2} = 59.16 \pm 5.25$ mV; $p < 0.05$). Slopes of the voltage-activation curve (i.e. voltage sensitivity) ($k =$
8 49.38 ± 2.03 mV WT, $k = 43.29 \pm 2.63$ mV A172V, $k = 45.20 \pm 2.36$ mV; $p = 0.18$) were not significantly
9 different.

10 g) Current-voltage relationships were tested with a voltage-ramp protocol in which voltage changes at a
11 steady rate and the resulting current is recorded. After administration of $25 \mu\text{M}$ (arrow) averaged currents
12 from voltage-ramps were extrapolated and at +90mV showed a three-fold increase in current densities at
13 positive potentials after application of $25 \mu\text{M}$ AITC (WT = 85.13 ± 23.30 mV, p.A172V = 250.4 ± 62.39 mV,
14 p.N855S = 256.1 ± 54.90 mV; $p < 0.05$). Insert shows example tracing.

15 WT – Wild Type

16 Data are presented as mean \pm SEM.

17 Statistical analysis for group comparisons - One way ANOVA with Sidak's multiple comparison test (* -
18 indicates statistically significant differences, $P < 0.05$)

19
20 219x350mm (300 x 300 DPI)
21
22
23
24
25
26
27
28
29
30
31
32
33
34
35
36
37
38
39
40
41
42
43
44
45
46
47
48
49
50
51
52
53
54
55
56
57
58
59
60

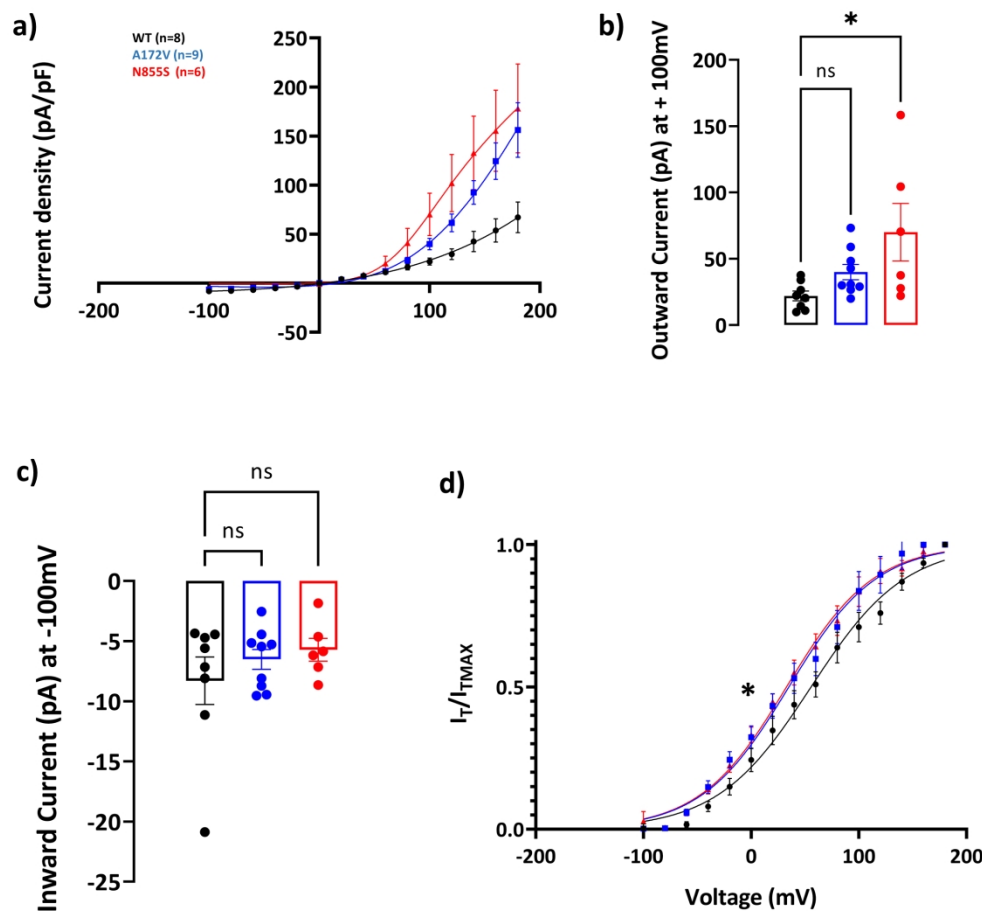


Figure 4

Figure 4:

Application of 100 μ M of Menthol in the presence of intracellular and extracellular calcium shows enhanced activity of p.A172V and p.N855S variants. Current-voltage curves were measured with a two voltage-step protocol (voltage-ramps ranging from -100 mV to + 100 mV for 500 ms, every 5 seconds; holding potential was set at -70 mV).

- a) Current density, assessed using a two-voltage step protocol, in WT and variant channels were significantly different as quantified in d) and e)
- b) Outward currents were enhanced for both p.A172V and p.N855S (+100mV, WT = 21.96 ± 3.64 mV, p.A172 = 39.94 ± 5.80 mV, and p.N855S = 70.07 ± 21.71 mV; $p < 0.05$)
- c) Inward currents were not statistically different (-100mV, WT = -8.29 ± 1.97 mV, -6.52 \pm 0.83mV p.A172V, and p.N855S = -5.72 ± 0.94 mV; $p = 0.58$, and $p = 0.40$, respectively)
- d) Half-maximal activation potential was significantly shifted leftward for p.A172V and p.N855S ($V_{1/2}$, WT= 61.83 ± 7.37 mV n = 8, p.A172V = 36.41 ± 7.58 mV n = 9, p.N855S = 33.60 ± 6.67 mV n = 6). Voltage sensitivity was significantly altered (slope factor $k = 41.51 \pm 2.33$ mV WT; 40.21 ± 2.98 mV p.A172V; 39.32 ± 3.03 mV p.N855S; $p < 0.05$).

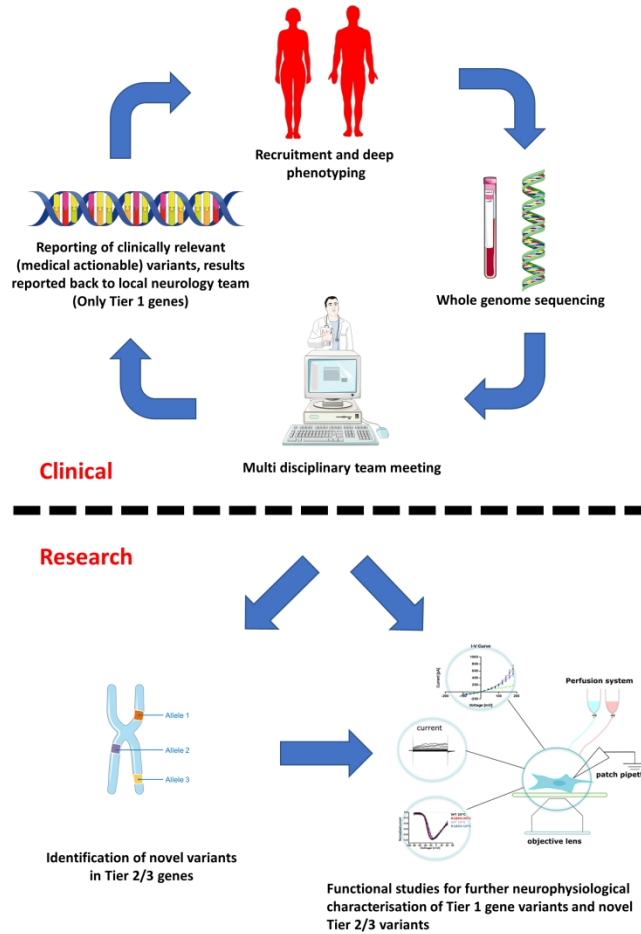
WT – Wild Type

Data are presented as mean \pm SEM.

Statistical analysis for group comparisons - One way ANOVA with Sidak's multiple comparison test (* - indicates statistically significant differences, $P < 0.05$)

1
2
3
4
5
6
7
8
9
10
11
12
13
14
15
16
17
18
19
20
21
22
23
24
25
26
27
28
29
30
31
32
33
34
35
36
37
38
39
40
41
42
43
44
45
46
47
48
49
50
51
52
53
54
55
56
57
58
59
60

199x199mm (300 x 300 DPI)

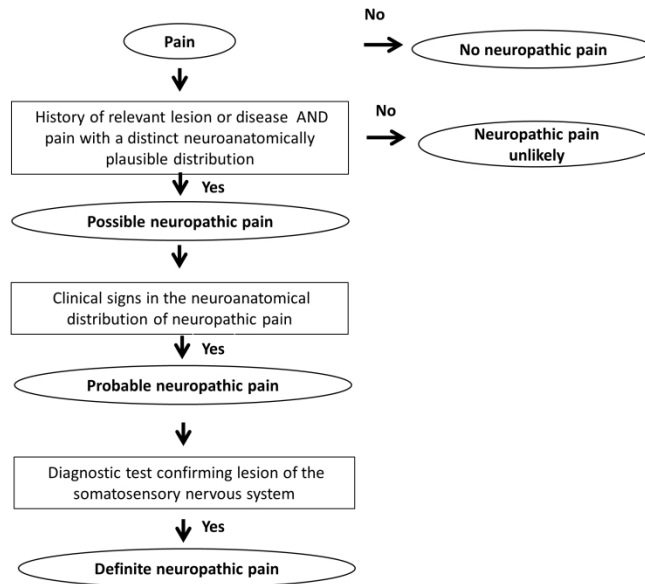


Supplementary Figure 1

Supplementary figure 1
 Flow diagram outlining recruitment of participants, analysis pipeline and genetic testing and the difference between the clinical reporting of relevant gene variants versus the exploratory gene analysis and in vitro functional assessment of variants of interest

190x338mm (300 x 300 DPI)

1
2
3
4
5
6
7
8
9
10
11
12
13
14
15
16
17
18
19
20
21
22
23
24
25
26
27
28
29
30
31
32
33
34
35
36
37
38
39
40
41
42
43
44
45
46
47
48
49
50
51
52
53
54
55
56
57
58
59
60



Supplementary Figure 2

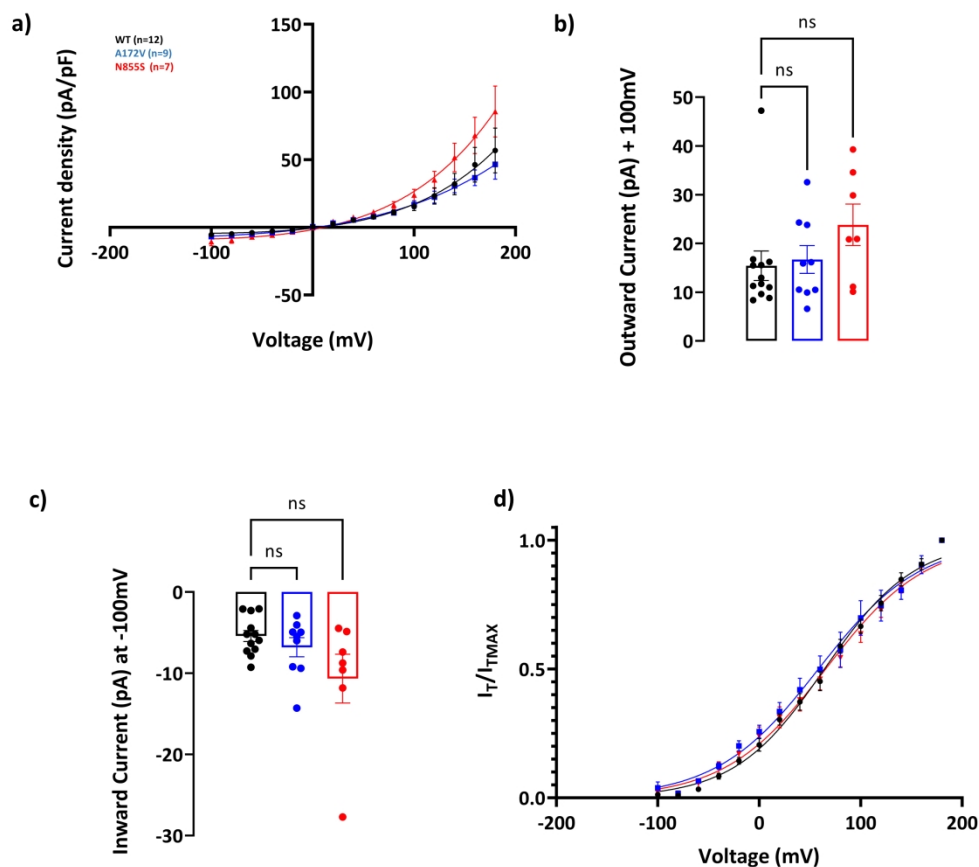
Supplementary figure 2
Flow diagram outlining neuropathic pain grading .
Possible neuropathic pain must fulfil criteria 1 and 2.
Probable neuropathic pain must fulfil criteria 1, 2 and 3.
Definite neuropathic pain must fulfil all 4 criteria.

1. Pain with a distinct neuroanatomically plausible distribution e.g. pain symmetrically distributed in the extremities, pain in erythematous areas
2. A history suggestive of a relevant lesion or disease affecting the peripheral or central somatosensory system e.g. a history of neuropathy symptoms including decreased sensation, or positive sensory symptoms e.g. burning, aching pain mainly in the toes, feet or legs.
3. Demonstration of distinct neuroanatomically plausible distribution of neuropathic pain e.g. presence of clinical signs of peripheral neuropathy such as decreased distal sensation or decreased/absent ankle reflexes.

1
2
3
4
5
6
7
8
9
10
11
12
13
14
15
16
17
18
19
20
21
22
23
24
25
26
27
28
29
30
31
32
33
34
35
36
37
38
39
40
41
42
43
44
45
46
47
48
49
50
51
52
53
54
55
56
57
58
59
60

4. Demonstration of the relevant lesion or disease by at least one confirmatory test e.g. abnormality on either nerve conduction tests, thermal thresholds or intra-epidermal nerve fibre density.

190x338mm (300 x 300 DPI)



Supplementary Figure 3

Supplementary figure 3

Biophysical characterisation of hTRPA1 WT, p.A172V and p.N855S variant in control conditions shows no significant differences. Voltage step protocol consisted of 400 ms voltage steps to test potentials ranging from -100 mV to $+180$ mV, followed by a final invariant step to -75 mV (400 ms to measure tail currents). The holding potential was set at -0 mV.

- a) Current density measured in WT and mutant channels were not statistically different as quantified in b) and c)
- b) Outward currents at ($+100$ mV, WT = 15.41 ± 3.01 pA/pF, p.A172V = 16.69 ± 2.85 pA/pF, N855S = 23.81 ± 4.25 pA/pF) were not significantly different between WT and the respective variants ($p = 0.77$ WT versus A71V2, $p = 0.17$ WT versus N855S)
- c) Inward currents (at -100 mV, WT = -5.42 ± 0.68 pA/pF, A172V = -6.80 ± 1.18 pA/pF and N855S = -10.66 ± 3.00 pA/pF), were not significantly different between WT and the respective variants ($p = 0.75$ WT versus A71V2, and $p = 0.05$ WT versus N855S).
- d) Voltage of half-maximal activation for WT $n = 12$, p.A172V $n = 9$ and p.N855S $n = 7$ ($V_{1/2}$, WT = 59.70 ± 4.59 mV, p.A172V = 59.45 ± 8.91 mV, p.N855S = 64.85 ± 8.09 mV; $p = 0.99$, and $p = 0.85$, respectively) and slopes of the voltage-activation curve (k , WT = 42.51 ± 2.01 mV, p.A172V = 46.19 ± 2.60 mV, p.N855S = 47.45 ± 1.88 mV; $p = 0.41$ and $p = 0.26$, respectively) were not statistically different.

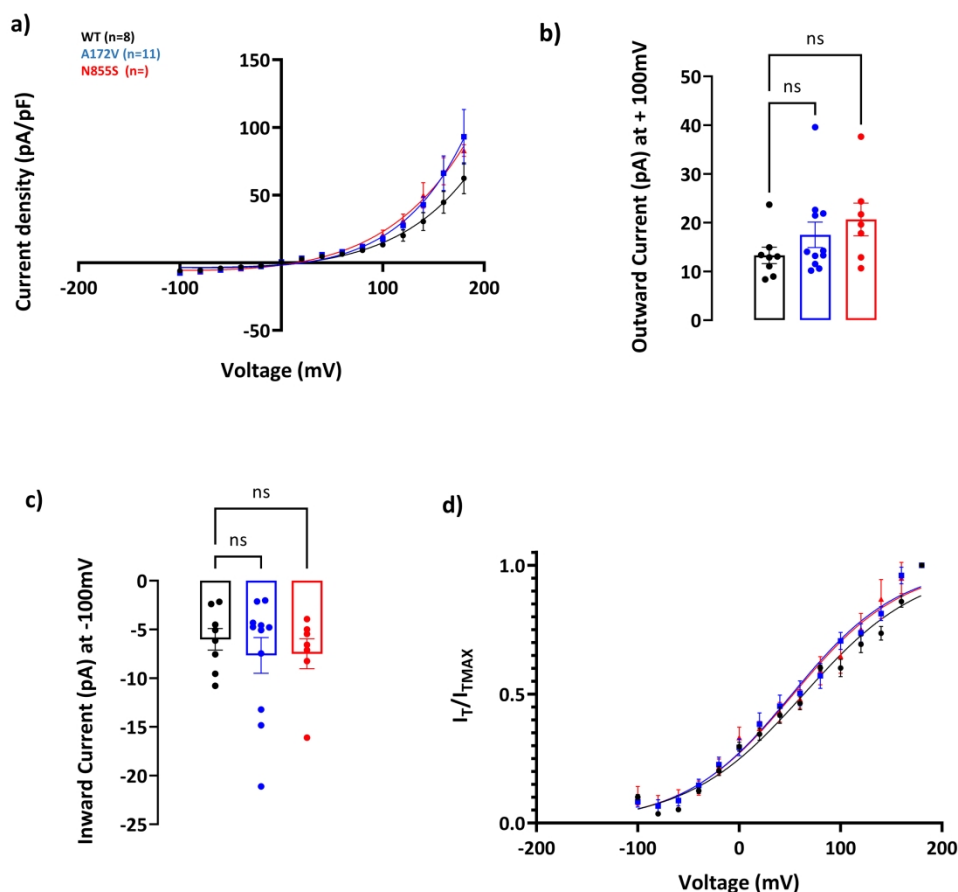
WT – Wild Type

Data are presented as mean \pm SEM.

1
2
3
4
5
6
7
8
9
10
11
12
13
14
15
16
17
18
19
20
21
22
23
24
25
26
27
28
29
30
31
32
33
34
35
36
37
38
39
40
41
42
43
44
45
46
47
48
49
50
51
52
53
54
55
56
57
58
59
60

Statistical analysis for group comparisons - One way ANOVA with Sidak's multiple comparison test (* - indicates statistically significant differences, P <0.05)

250x250mm (300 x 300 DPI)



Supplementary Figure 4

Supplementary figure 4:

Application of 100 μ M of Menthol, with extracellular calcium alone, did not alter p.A172V nor p.N855S channel excitability. Voltage-dependence activation of hTRPA1 p.A172V and p.N855S was measured in response to Menthol. Current-voltage curves were measured with a two voltage-step protocol (voltage-ramps ranging from -100 mV to + 100 mV for 500 ms, every 5 seconds; holding potential was set at -70 mV).

- a) Current densities were not statistically different for the variant channels when compared to WT as quantified in b) and c)
- b) Outward current (at +100mV, WT = 13.29 ± 1.69 pA/pF, p.A172V = 17.51 ± 2.60 pA/pF, p.N855S = 20.66 ± 3.35 pA/pF) were not significantly different ($p = 0.44$, and $p = 0.15$, respectively).
- c) Inward currents (at -100mV, WT = -6.02 ± 1.11 pA/pF, p.A172V = -7.66 ± 1.83 pA/pF, p.N855S = -7.49 ± 1.53 pA/pF) were not significantly different ($p = 0.72$, $p = 0.80$, respectively).
- d) Half-maximal activation voltage for WT $n = 8$, p.A172V $n = 8$, and N855S $n = 7$ ($V_{1/2}$, WT = 65.39 ± 5.79 mV, p.A172V = 56.61 ± 9.25 mV, p. N855S = 58.62 ± 7.31 mV, $p = 0.69$, and $p = 0.83$, respectively) were not statistically different. Slopes of the voltage-activation curve ($k = 56.66 \pm 1.40$ mV WT, 49.01 ± 1.53 mV p.A172V, 49.73 ± 3.28 mV N855S, $p = 0.022$ and $p = 0.069$, respectively) were reduced for both p.A172V and p.N855S.

WT – Wild Type

Data are presented as mean \pm SEM.

1
2
3
4
5
6
7
8
9
10
11
12
13
14
15
16
17
18
19
20
21
22
23
24
25
26
27
28
29
30
31
32
33
34
35
36
37
38
39
40
41
42
43
44
45
46
47
48
49
50
51
52
53
54
55
56
57
58
59
60

Statistical analysis for group comparisons - One way ANOVA with Sidak's multiple comparison test (* - indicates statistically significant differences, $P < 0.05$).

250x250mm (300 x 300 DPI)

Table 1

<u>NPD</u>	<u>Diagnostic criteria</u>	<u>Associated phenotypes</u>	<u>Likely inheritance</u>	<u>Known gene (OMIM #)</u>	<u>PMID reference</u>
Congenital insensitivity to pain (including Hereditary sensory and autonomic neuropathy type IV, V, VII)	Inability to perceive painful stimuli Other somatosensory modalities may be impaired but the predominant clinical presentation is loss of pain sensibility	Anosmia Autonomic dysfunction Anhydrosis Intellectual impairment	AD, AR	SCN9A (243000), NGF (608654), NTRK1 (256800), SCN11A (615548), PRDM12 (616488), MPV17 (256810), CLTCL1 (601273)	17167479, 17470132, 17597096, 23596073, 19304393, 14976160, 8696348, 24036948, 26005867, 185990, 26068709
Hereditary sensory and autonomic neuropathy type I, II, III	Progressive neuropathies where the presenting or predominant feature is altered sensory function	Autonomic features and motor nerve involvement	AD, AR, X-linked	SPLTLC1 (162400), SPTLC2 (605713), WNK1 (201300), RAB7 (600882), IKBKAP (223900), FAM134B (613115), KIF1A (614213), ATL1 (613708), ATL3 (615632), CCT5 (256840)	11242114, 20920666, 15060842, 12545426, 8102296, 19838196, 21820098, 21194679, 24459106, 16399879
Erythromelalgia	Pain and erythema of the extremities which is exacerbated by warming and relieved by cooling. Initially episodic but may become persistent.	Onset by age 20	AD	SCN9A (133020)	14985375
Familial episodic pain syndrome	Severe episodic pain usually localised to the trunk and limbs with no structural cause. Triggers include cold environment, exercise and fasting.	Onset usually in childhood Possible family history	AD	TRPA1 (615040) , SCN11A (615552)	20547126, 24207120
Small fibre neuropathy	Probable—symptoms in hands and feet consistent with small fibre dysfunction (pain and altered temperature sensibility), clinical signs of small fibre damage (reduced pin prick sensitivity and ability to discriminate warm/cool) and normal nerve conduction studies. Definite—symptoms in hands and feet, clinical signs of small fibre damage, normal nerve conduction studies, and altered intra-epidermal nerve fibre density at the ankle and/or abnormal quantitative sensory testing of thermal thresholds at the foot	Autonomic features	AD	SCN9A (133020), SCN10A (615551), SCN11A (615552)	21698661, 23115331, 24207120
Post traumatic neuropathy	Traumatic nerve injury with clinical evidence of nerve injury in the neuroanatomical distribution of neuropathic pain		N/A	N/A	
Neuropathic pain NOS	Pain with a distinct neuroanatomically plausible distribution; however, no evidence of nerve injury found on clinical examination or specialised investigations		N/A	N/A	

Table 1

Table 2

Gene symbol	HGNC database: ID	Chromosomal position	HGNC database: description	Clinical phenotypes	OMIM	PMID Reference
Tier 1 genes						
FAM134B	25964	5p15.1	family with sequence similarity 134 member B	HSAN 2B;	613115	19838196, 21115472, 24327336
IKBKAP	5959	9q31	inhibitor of kappa light polypeptide gene enhancer in B-cells, kinase complex-associated protein	Riley Day Syndrome/HSAN 3/Familial Dysautonomia	223900	8102296, 11179021, 11179008
NGF	7808	1p13.1	nerve growth factor	HSAN 5	608654	14976160, 20978020
NTRK1	8031	1q21-q22	neurotrophic receptor tyrosine kinase 1	HSAN 4/Congenital insensitivity to pain with anhidrosis	256800	8696348, 11668614, 18077166
PRDM12	13997	9q34.12	PR domain 12	HSAN 8/Congenital insensitivity to pain	616488	26005867, 26975306
RAB7	9788	3q21	RAB7A, member RAS oncogene family	HSAN1/2B	600882	12545426,
SCN9A	10597	2q24.3	sodium voltage-gated channel alpha subunit 9	Congenital insensitivity to pain, primary erythromelalgia, paroxysmal extreme pain disorder	243000, 133020	17167479, 14985375, 17145499
SCN10A	10582	3p22.2	sodium voltage-gated channel alpha subunit 10	Painful small fibre neuropathy	615551	23115331, 24006052, 26711856
SCN11A	10583	3p22.2	sodium voltage-gated channel alpha subunit 11	Familial episodic pain; Insensitivity to pain	615552, 615548	24036948, 24207120, 24776970
SEPT9	7323	17q25.3	septin 9	Hereditary neuralgic amyotrophy	162100	16186812, 19451530, 21556032
SPTLC1	11277	9q22.31	serine palmitoyltransferase long chain base subunit 1	HSAN 1	162400	11242114, 11242106, 15037712,
SPTLC2	11278	14q24.3	serine palmitoyltransferase long chain base subunit 2	HSAN 1	605713	12207934, 20920666, 23658386
TTR	12405	18q12.1	transthyretin	Familial amyloidosis	105210	3011930, 14640030
WNK1	14540	12p13.3	WNK lysine deficient protein kinase 1	HSAN 2	201300	15060842, 18521183, 21625937
Tier 2 genes						
<i>ATL1</i>	HGNC:11231	14q21.3	atlastin GTPase 1	HSAN 1; Hereditary Spastic Paraplegia	613708	21194679, 22340599
<i>ATL3</i>	HGNC:24526	11q13.1	atlastin GTPase 3	HSAN 1	615632	24459106, 30680846
<i>CCT5</i>	HGNC:1618	5p15.2	chaperonin containing TCP1 subunit 5	HSAN with spastic paraplegia	256840	16399879
<i>CLTCL1</i>	HGNC:2093	22q11.2	clathrin heavy chain like 1	HSAN 5/Congenital insensitivity to pain	601273	26068709
<i>KIF1A</i>	HGNC:888	2q37.2	kinesin family member 1A	HSAN 2; Hereditary Spastic Paraplegia	614213	21820098, 25265257

<i>MPV17</i>	HGNC:7224	2p23.3	MPV17, mitochondrial inner membrane protein	Congenital neuropathy leads to absent pain at birth in severe cases. Hepatic failure and encephalopathy overshadow the neuropathy.	256810	185990, 11431741
<i>NAGLU</i>	HGNC:7632	17q21.2	N-acetyl-alpha-glucosaminidase	Painful axonal polyneuropathy in heterozygotes; mucopolysaccharidosis IIIB when homozygous		25818867
<i>TRPA1</i>	HGNC:497	8q13	transient receptor potential cation channel subfamily A member 1	Familial episodic pain syndrome	615040	20547126,16564016
Tier 3 genes						
<i>KCNA1</i>	HGNC:6218	12p13	potassium voltage-gated channel subfamily A member 1			20724292
<i>KCNS1</i>	HGNC:6300	20q12	potassium voltage-gated channel modifier subfamily S member 1	No specific Mendelian disorder but the rs734784 allele enhances risk of nerve pain following nerve injury		
<i>TRPM8</i>	HGNC:17961	2q37	transient receptor potential cation channel subfamily M member 8			
<i>TRPV1</i>	HGNC:12716	17p13.2	transient receptor potential cation channel subfamily V member 1			9349813, 9768840
<i>TRPV2</i>	HGNC:18082	17p11.2	transient receptor potential cation channel subfamily V member 2			
<i>TRPV3</i>	HGNC:18084	17p13.3	transient receptor potential cation channel subfamily V member 3			
<i>TRPV4</i>	HGNC:18083	12q24.11	transient receptor potential cation channel subfamily V member 4			
<i>SCN8A</i>	HGNC:10596	12q13.1	sodium voltage-gated channel alpha subunit 8			22493249
<i>SETDB2</i>	HGNC:20263	13q14	SET domain bifurcated 2	Mutation identified in this group: HSN/Insensitivity to pain (unpublished data DLB)		
Additional genes after contemporaneous search						
<i>DNMT1</i>	HGNC:2976	19p13.2	DNA methyltransferase 1	Neuropathy, hereditary sensory, type IE	126375	21532572, 23365052, 25678562
<i>Dystonin</i>	HGNC:1090	6p12.1	Cytoskeleton linker protein	hereditary sensory and autonomic neuropathy type VI (HSAN6)	614653	22522446
<i>ZFX2</i>	HGNC:20152	14q11.2	zinc finger homeobox 2	Congenital insensitivity to pain Marsili syndrome (MARSIS)	243000	29253101
<i>FAAH</i>	HGNC:50679	1p33	fatty acid amide hydrolase pseudogene 1	Insensitivity to pain	243000	30929760
<i>FLVCR1</i>	HGNC:24682	1q32.3	FLVCR heme transporter 1	Sensory neurodegeneration with loss of pain perception	609144	27923065

Table 2

Table 3

Page No	Clinical phenotype	Neuropathic pain grading	Gene	Nucleotide change	Amino acid change	Assigned pathogenicity	The frequency of variants in databases				In silico analysis		Previous study demonstrating altered channel function (PMID Reference)
							gnomAD	WGS10K	NPD European (African)	NIHR Bioresources controls European (African)	SIFT score	Polyphen	
1													
2													
3													
4													
5													
6													
7	Erythromelalgia	Definite	SCN9A	c.2543T>C	p.Ile848Thr p.I848T	Clearly pathogenic	.	0.0001	0.0039 (0)	0 (0)	0.00	probably damaging	Yes (15385606)
8	Erythromelalgia	Definite	SCN9A	c.2543T>C	p.Ile848Thr p.I848T	Clearly pathogenic	.	0.0001	0.0039 (0)	0 (0)	0.00	probably damaging	Yes (15385606)
9													
10	Sensorimotor neuropathy	Probable	SPTLC1	c.399T>G	p.Cys133Trp p.C133W	Clearly pathogenic	.	0.0000	0.0039 (0)	0 (0)	0.00	probably damaging	Yes (16210380)
11	Small fibre neuropathy	Definite	SCN10A	c.4984G>A	p.Gly1662Ser p.G1662S	Likely pathogenic	0.0014	0.0010	0.0039 (0)	0.0005 (0)	0.00	probably damaging	Yes (23115331)
12	Small fibre neuropathy	Definite	SCN11A	c.4628G>A	p.Cys1543Tyr p.C1543Y	Likely pathogenic	0.0001	0.00004	0.0039 (0.0131)	0 (0)	0.01	probably damaging	No studies for this variant
13													
14	Painful sensory neuropathy	Definite	SPTLC2	c.886A>C	p.Ile296Leu p.I296L	VUS	.	0.0000	0.0039 (0)	0 (0)	0.04	possibly damaging	No studies for this variant
15													
16	Non-freezing cold injury	Definite	SCN9A	c.554G>A	p.Arg185His p.R185H	VUS	0.0031	0.0016	0 (0.0921)	0.0015 (0.0064)	0.01	probably damaging	Yes (21698661, 22826602)
17													
18	Non-freezing cold injury	Definite	SCN9A	c.554G>A	p.Arg185His p.R185H	VUS	0.0031	0.0016	0 (0.0921)	0.0015 (0.0064)	0.01	probably damaging	Yes (21698661, 22826602)
19	Non-freezing cold injury	Definite	SCN9A	c.554G>A	p.Arg185His p.R185H	VUS	0.0031	0.0016	0 (0.0921)	0.0015 (0.0064)	0.01	probably damaging	Yes (21698661, 22826602)
20													
21	Non-freezing cold injury	Definite	SCN9A	c.554G>A	p.Arg185His p.R185H	VUS	0.0031	0.0016	0 (0.0921)	0.0015 (0.0064)	0.01	probably damaging	Yes (21698661, 22826602)
22													
23	Non-freezing cold injury	Definite	SCN9A	c.554G>A	p.Arg185His p.R185H	VUS	0.0031	0.0016	0 (0.0921)	0.0015 (0.0064)	0.01	probably damaging	Yes (21698661, 22826602)
24	Non-freezing cold injury	Definite	SCN9A	c.554G>A	p.Arg185His p.R185H	VUS	0.0031	0.0016	0 (0.0921)	0.0015 (0.0064)	0.01	probably damaging	Yes (21698661, 22826602)
25													
26	Small fibre neuropathy	Definite	SCN9A	c.4612T>C	p.Trp1538Arg p.W1538R	VUS	0.0020	0.0018	0.0039 (0)	0.0018 (0)	0.71	benign	Yes (23292638)
27	Small fibre neuropathy	Definite	SCN9A	c.1445A>G	p.K482R p.Lys482Arg	VUS	0	0.00004	0.0039 (0)	0 (0)	0.18	benign	No studies for this variant
28													
29	Small fibre neuropathy	Probable	SCN9A	c.2215A>G	p.Ile739Val p.I739V	VUS	0.0024	0.0032	0.0078 (0)	0.0041 (0)	0.03	benign	Yes (22826602)
30	Small fibre neuropathy	Definite	SCN9A	c.2215A>G	p.Ile739Val p.I739V	VUS	0.0024	0.0032	0.0078 (0)	0.0041 (0)	0.03	benign	Yes (22826602)
31													
32	Painful sensory neuropathy	Probable	SCN9A	c.2215A>G	p.Ile739Val p.I739V	VUS	0.0024	0.0032	0.0078 (0)	0.0041 (0)	0.03	benign	Yes (22826602)
33													
34	Sensorimotor neuropathy	Definite	SCN9A	c.2215A>G	p.Ile739Val p.I739V	VUS	0.0024	0.0032	0.0078 (0)	0.0041 (0)	0.03	benign	Yes (22826602)
35	Small fibre neuropathy	Definite	SCN9A	c.4982A>G	p.Glu1661Gly p.E1661G	VUS	0.0000	0.0001	0.0039 (0)	0.0018 (0)	0.10	benign	No studies for this variant
36													
37	Traumatic neuropathy	Probable	SCN9A	c.554G>A	p.Arg185His p.R185H	VUS	0.0031	0.0016	0 (0.0921)	0.0015 (0.0064)	0.01	probably damaging	Yes (21698661, 22826602)
38													
39	Painful Sensory neuropathy	Definite	SCN10A	c.3445G>A	p.V1149M p.Pro1149Met	VUS	0.0001	0.0003	0.0039 (0)	0.00008 (0)	0.00	probably damaging	No studies for this variant
40	Small fibre neuropathy	Definite	SCN10A	c.2428G>T	p.Gly810Trp p.G810W	VUS	0.0003	0.0005	0.0039 (0)	0.0004 (0)	0.00	probably damaging	No studies for this variant

23	Painful Sensory neuropathy	Definite	SCN10A	c.2737G>A	p.Ala913Thr p.A913T	VUS	0.0003	0.0006	0.0039 (0)	0.0003 (0)	0.01	probably damaging	No studies for this variant
24	Erythromelalgia	Probable	SCN10A	c.968A>G	p.Y323Cp.Tyr323Cys	VUS	.	0.00004	0.0039 (0)	0 (0)	0.00	probably damaging	No studies for this variant
125	Small fibre neuropathy	Definite	SCN11A	c.2471A>G	p.Glu824Glyp.E824G	VUS	.	0.00004	0.0039 (0)	0 (0)	0.02	possibly damaging	No studies for this variant
226	Episodic pain	Possible	SCN11A	c.1730C>T	p.P577Lp.Pro577Leu	VUS	0.0002	0.0006	0.0039 (0)	0.0005 (0)	0.00	probably damaging	No studies for this variant

Table 3

For Review Only

Table 4

Genomic coordinates and the HGNC gene symbol for gene models	Fraction with rare variants	Number of variants considered	P Value	Rho
Europeans				
Tier 1 pain genes				
All Neuropathic pain (n=126) vs Controls (n=5096)				
1:115828713-115836247_NGF	0.0026346	14	2.053e-08	0
3:38387651-39150434_SCN11A_promoter	0.0037214	186	1.7809e-06	0
Tier 2-3 pain genes				
All Neuropathic pain vs Controls				
1:212733740-213037331_FLVCR1_promoter	0.07838	704	1.0404e-05	0
2:241653459-241759532_KIF1A	0.038202	180	8.74e-08	0
2:241757820-241808205_KIF1A_promoter	0.011691	182	1.5858e-06	0
12:52056606-52201160_SCN8A	0.0097151	44	5.0888e-08	0
2:234835229-234916724_TRPM8	0.017948	90	2.9788e-06	0
Tier 1-3 pain genes				
Probable/Definite Neuropathic pain vs Controls				
1:212733740-213037331_FLVCR1_promoter	0.078509	704	2.0274e-07	0
2:241656788-241737150_KIF1A	0.038265	180	2.7235e-09	0
2:241757820-241808205_KIF1A_promoter	0.01171	182	2.4975e-07	0
1:115828713-115836247_NGF	0.002639	14	2.6429e-09	0
12:52056606-52201160_SCN8A	0.0097312	44	1.5018e-09	0
2:167227721-167351474_SCN9A_promoter	0.037605	461	2.3805e-05	0
8:72935185-72987631_TRPA1	0.015009	73	5.2482e-05	0
2:234835229-234916724_TRPM8	0.017978	90	2.825e-07	0
SCN9A, SCN10A, SCN11A functionally validated variants				
3:38739727-38793804_SCN10A (Small fibre neuropathy)	0.0013329	2	0.00016219	0

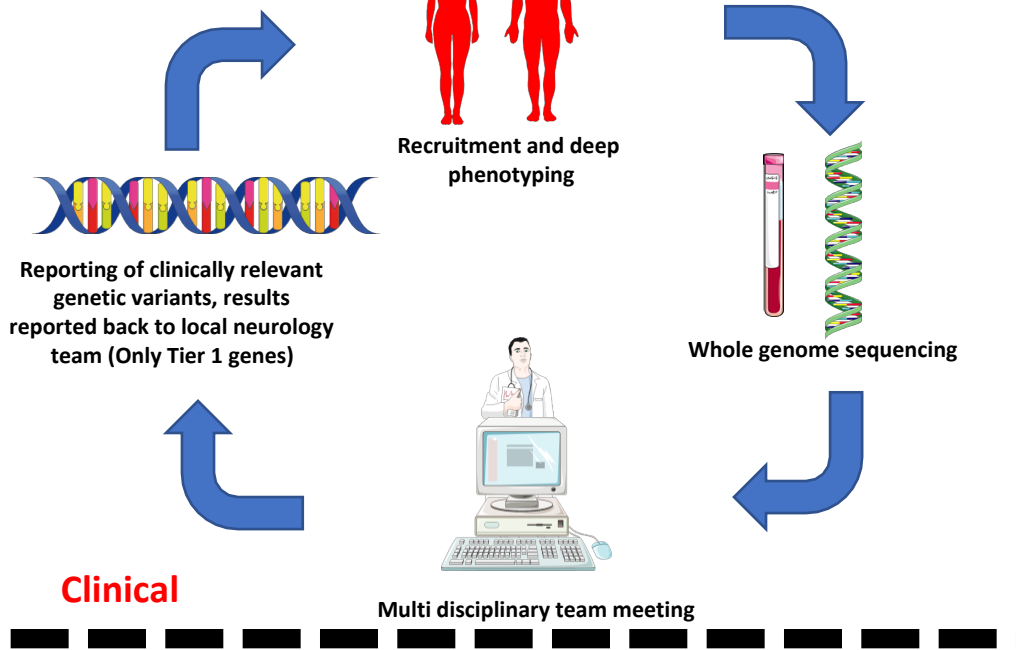
Table 4

Supplementary table 1

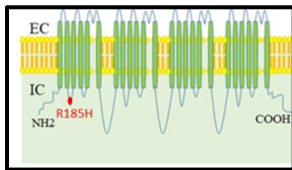
Genomic coordinates and the HGNC gene symbol for gene models	Fraction with rare variants	Variants considered	P Value	Rho
Tier 1-3 pain genes				
Europeans				
Probable/Definite Neuropathic pain vs Controls				
1:212733740-213037331_FLVCR1_promoter	0.078509	704	2.0274e-07	0
2:241656788-241737150_KIF1A	0.038265	180	2.7235e-09	0
2:241757820-241808205_KIF1A_promoter	0.01171	182	2.4975e-07	
1:115828713-115836247_NGF	0.002639	14	2.6429e-09	0
12:52056606-52201160_SCN8A	0.0097312	44	1.5018e-09	0
2:167227721-167351474_SCN9A_promoter	0.037605	461	2.3805e-05	0
8:72935185-72987631_TRPA1	0.015009	73	5.2482e-05	0
2:234835229-234916724_TRPM8	0.017978	90	2.825e-07	0
Possible Neuropathic pain vs Controls				
5:10237637-10311587_CCT5_promoter	0.043829	390	2.1646e-10	0
22:19158112-19468896_CLTCL1_promoter	0.12628	755	1.8541e-05	0
2:27272295-27888854_MPV17_promoter	0.14408	1039	1.1537e-06	0
9:132888940-133713656_PRDM12_promoter	0.12242	778	2.5937e-24	0
3:38887266-38992020_SCN11A	0.022166	116	3.2814e-17	0
3:38387651-39150434_SCN11A_promoter	0.036776	182	9.13e-36	0
2:167051740-167168308_SCN9A	0.031066	138	1.0185e-11	0
9:94179481-95733983_SPTLC1_promoter	0.17162	1253	1.4402e-20	0
14:77972340-78045374_SPTLC2	0.023678	113	7.4671e-17	0
17:16188184-16396312_TRPV2_promoter	0.16927	1239	2.8037e-07	0
14:23990197-24004569_ZFHX2	0.037615	195	1.8008e-11	0
Idiopathic vs Controls				
9:111694228-111884278_ELP1_promoter	0.099514	665	0.00010639	0
1:212733740-213037331_FLVCR1_promoter	0.078238	689	3.5673e-11	0
9:111637167-111693371_IKKBKAP	0.021612	98	6.0954e-14	0
2:27532377-27548436_MPV17	0.0065338	31	2.3621e-11	0
2:27272295-27888854_MPV17_promoter	0.14492	1039	1.8079e-11	0
17:40688345-40696166_NAGLU	0.0065338	31	2.5867e-11	0
1:156735601-156831188_NTRK1_promoter	0.053443	606	1.2915e-12	0
3:38387651-39150434_SCN11A_promoter	0.03669	181	7.875e-07	0
12:52056606-52201160_SCN8A	0.0093818	42	7.6272e-10	0
2:167227721-167351474_SCN9A_promoter	0.03736	445	3.7788e-07	0
9:94794766-94877614_SPTLC1	0.0073714	41	2.0265e-12	0
8:72935185-72987631_TRPA1	0.01491	72	2.1457e-10	0
Non-freezing cold injury vs Controls				
11:62605687-64041758_ATL3_promoter	0.2605	1807	1.9334e-26	0
22:19158112-19468896_CLTCL1_promoter	0.12622	755	1.7755e-11	0
6:56322787-56765386_DST	0.064706	326	7.2668e-21	0
2:241653211-241737219_KIF1A	0.037479	174	2.6565e-24	0
2:27272295-27888854_MPV17_promoter	0.14437	1036	2.418e-05	0
1:115828571-115836350_NGF	0.002521	13	6.9657e-126	0
1:115257831-115881445_NGF_promoter	0.073613	415	9.0969e-55	0
12:51791830-52209151_SCN8A_promoter	0.073613	593	5.8951e-06	0
9:94179481-95733983_SPTLC1_promoter	0.17143	1244	5.4476e-30	0
14:77768191-78083941_SPTLC2_promoter	0.06084	683	1.1154e-26	0
2:234825742-235408070_TRPM8_promoter	0.058824	421	9.7579e-49	0
12:109567961-110487716_TRPV4_promoter	0.16185	898	1.6927e-12	0
Erythromelalgia vs Controls				
5:10254263-10266494_CCT5	0.013754	63	1.1515e-09	0
19:9647679-11208553_DNMT1_promoter	0.44918	3552	5.0184e-07	0
6:56322787-56765386_DST	0.064743	328	9.2064e-09	0
9:111694228-111884278_ELP1_promoter	0.099631	660	2.6704e-12	0

1:212733740-213037331_FLVCR1_promoter	0.078665	695	4.5875e-62	0
12:5020374-5027410_KCNA1	0.022979	114	8.8721e-09	0
20:43720954-43728938_KCNS1	0.016437	79	5.6901e-10	0
20:43593848-44003217_KCNS1_promoter	0.046964	245	6.3713e-22	0
2:241653211-241737219_KIF1A	0.037571	174	9.983e-40	0
2:27272295-27888854_MPV17_promoter	0.14425	1040	4.0699e-07	0
1:115257831-115881445_NGF_promoter	0.073465	414	4.0189e-19	0
3:38738320-38835432_SCN10A	0.024992	117	2.745e-08	0
12:52078070-52202289_SCN8A	0.0093928	42	6.9227e-19	0
2:167051740-167168308_SCN9A	0.03103	138	0.00011167	0
17:75303232-75496662_SEPT9	0.020798	92	9.6699e-10	0
17:74347488-75883645_SEPTIN9_promoter	0.68031	14656	2.0928e-23	0
9:94179481-95733983_SPTLC1_promoter	0.17159	1249	1.658e-17	0
2:234835229-234928166_TRPM8	0.017612	88	5.975e-10	0
12:936533-1020561_WNK1	0.030191	130	9.9286e-06	0
Post Traumatic Neuropathy vs controls				
14:50777141-51327966_ATL1_promoter	0.094511	689	3.6407e-14	0
11:62605687-64041758_ATL3_promoter	0.2607	1807	7.2586e-06	0
19:9647679-11208553_DNMT1_promoter	0.44972	3553	2.0827e-11	0
1:46215085-47268057_FAAH_promoter	0.10307	553	5.4233e-06	0
9:111629802-111693471_IKBKAP	0.021655	96	1.8508e-18	0
20:43720954-43728938_KCNS1	0.016451	79	1.9211e-10	0
2:241653211-241737219_KIF1A	0.037771	176	2.0856e-38	0
9:132888940-133713656_PRDM12_promoter	0.12187	777	4.1157e-06	0
3:38387651-39150434_SCN11A_promoter	0.036596	182	7.715e-09	0
12:51791830-52209151_SCN8A_promoter	0.073527	596	4.1392e-20	0
2:234835229-234928166_TRPM8	0.017626	88	1.6971e-24	0
18:29077164-29267441_TTR_promoter	0.077052	399	2.057e-07	0
12:678629-1060004_WNK1_promoter	0.1296	1229	3.4161e-11	0
Neuropathic Pain Not Otherwise Specified vs controls				
5:10237637-10311587_CCT5_promoter	0.043807	390	1.7269e-05	0
6:56322787-56765386_DST	0.064787	328	1.2338e-16	0
1:212733740-213037331_FLVCR1_promoter	0.078214	689	3.2979e-10	0
1:115257831-115881445_NGF_promoter	0.073347	411	5.1011e-05	0
1:156735601-156831188_NTRK1_promoter	0.053206	606	4.9332e-07	0
9:132888940-133713656_PRDM12_promoter	0.12219	777	5.1652e-10	0
3:38387651-39150434_SCN11A_promoter	0.036925	183	1.1968e-45	0
12:52078070-52202289_SCN8A	0.0093991	41	9.7448e-23	0
2:167051740-167168308_SCN9A	0.031051	137	1.1055e-07	0
2:167227721-167351474_SCN9A_promoter	0.037261	441	1.2761e-07	0
9:94179481-95733983_SPTLC1_promoter	0.17153	1253	9.4963e-18	0
14:77972340-78045374_SPTLC2	0.023666	113	4.924e-13	0
Africans				
Post Traumatic Neuropathy vs controls				
6:56323823-56819337_DST	0.076923	14	8.3758e-05	0
Small Fibre Neuropathy vs controls				
2:241653211-241737219_KIF1A	0.044586	7	1.9638e-06	0
2:234835229-234928166_TRPM8	0.044586	7	6.7973e-06	0
12:936533-1020561_WNK1	0.031847	5	0.00010244	0
12:678629-1060004_WNK1_promoter	0.17834	64	6.2972e-06	0
Non-freezing cold injury vs Controls				
1:156811877-156851636_NTRK1	0.02139	4	7.1487e-09	0

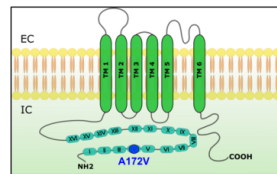
Supplementary table 1



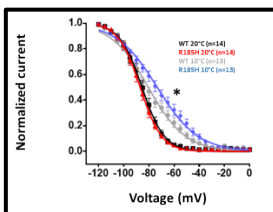
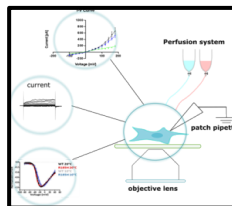
Increase frequency of *SCN9A* p.Arg185His in patients with non-freezing cold injury



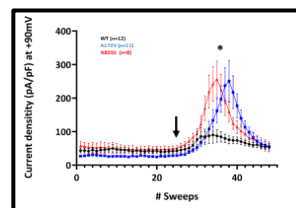
Identification of novel *TRPA 1* variant p.Ala172Val in episodic pain disorder



Patch clamp analysis



Gain of function of $Na_v1.7$ after cooling (the environmental trigger for non-freezing cold injury)



Gain of *TRPA 1* channel function in response to agonist stimulation.

1
2
3 **Abbreviated summary**
4

5 ‘Whole genome sequencing revealed clinically relevant variants in 12% of participants with
6 extreme neuropathic pain disorders. The majority of variants were in ion channels including
7 new phenotype associations (*SCN9A* p.Arg185His and non-freezing cold injury) and novel gain
8 of function variants (*TRPA1* p.Ala172Val and episodic pain).’
9
10
11
12
13
14
15
16
17
18
19
20
21
22
23
24
25
26
27
28
29
30
31
32
33
34
35
36
37
38
39
40
41
42
43
44
45
46
47
48
49
50
51
52
53
54
55
56
57
58
59
60

For Review Only

STROBE Statement—checklist of items that should be included in reports of observational studies

	Item No.	Recommendation	Page No.	Relevant text from manuscript
Title and abstract	1	(a) Indicate the study's design with a commonly used term in the title or the abstract		
		(b) Provide in the abstract an informative and balanced summary of what was done and what was found	3	
Introduction				
Background/rationale	2	Explain the scientific background and rationale for the investigation being reported	4	
Objectives	3	State specific objectives, including any prespecified hypotheses	4	
Methods				
Study design	4	Present key elements of study design early in the paper	5-10	
Setting	5	Describe the setting, locations, and relevant dates, including periods of recruitment, exposure, follow-up, and data collection	5	
Participants	6	(a) <i>Cohort study</i> —Give the eligibility criteria, and the sources and methods of selection of participants. Describe methods of follow-up <i>Case-control study</i> —Give the eligibility criteria, and the sources and methods of case ascertainment and control selection. Give the rationale for the choice of cases and controls <i>Cross-sectional study</i> —Give the eligibility criteria, and the sources and methods of selection of participants	5, table 1	
		(b) <i>Cohort study</i> —For matched studies, give matching criteria and number of exposed and unexposed <i>Case-control study</i> —For matched studies, give matching criteria and the number of controls per case		
Variables	7	Clearly define all outcomes, exposures, predictors, potential confounders, and effect modifiers. Give diagnostic criteria, if applicable	5-10	
Data sources/ measurement	8*	For each variable of interest, give sources of data and details of methods of assessment (measurement). Describe comparability of assessment methods if there is more than one group	5-10	
Bias	9	Describe any efforts to address potential sources of bias	5-10	
Study size	10	Explain how the study size was arrived at	Not applicable	

Continued on next page

Quantitative variables	11	Explain how quantitative variables were handled in the analyses. If applicable, describe which groupings were chosen and why	5-10	
Statistical methods	12	(a) Describe all statistical methods, including those used to control for confounding	6,7,10	
		(b) Describe any methods used to examine subgroups and interactions	5-10	
		(c) Explain how missing data were addressed	Not applicable	
		(d) <i>Cohort study</i> —If applicable, explain how loss to follow-up was addressed <i>Case-control study</i> —If applicable, explain how matching of cases and controls was addressed <i>Cross-sectional study</i> —If applicable, describe analytical methods taking account of sampling strategy	6-8	
		(e) Describe any sensitivity analyses		
Results				
Participants	13*	(a) Report numbers of individuals at each stage of study—eg numbers potentially eligible, examined for eligibility, confirmed eligible, included in the study, completing follow-up, and analysed	11	
		(b) Give reasons for non-participation at each stage	Figure 1	
		(c) Consider use of a flow diagram	Figure 1	
Descriptive data	14*	(a) Give characteristics of study participants (eg demographic, clinical, social) and information on exposures and potential confounders	11-14	
		(b) Indicate number of participants with missing data for each variable of interest		
		(c) <i>Cohort study</i> —Summarise follow-up time (eg, average and total amount)		
Outcome data	15*	<i>Cohort study</i> —Report numbers of outcome events or summary measures over time		
		<i>Case-control study</i> —Report numbers in each exposure category, or summary measures of exposure		
		<i>Cross-sectional study</i> —Report numbers of outcome events or summary measures	Table 2, 11-14	
Main results	16	(a) Give unadjusted estimates and, if applicable, confounder-adjusted estimates and their precision (eg, 95% confidence interval). Make clear which confounders were adjusted for and why they were included	Figure 2-4; table	
		(b) Report category boundaries when continuous variables were categorized		
		(c) If relevant, consider translating estimates of relative risk into absolute risk for a meaningful time period		

Continued on next page

Other analyses	17	Report other analyses done—eg analyses of subgroups and interactions, and sensitivity analyses	11-12	
Discussion				
Key results	18	Summarise key results with reference to study objectives	15	
Limitations	19	Discuss limitations of the study, taking into account sources of potential bias or imprecision. Discuss both direction and magnitude of any potential bias	15-18	
Interpretation	20	Give a cautious overall interpretation of results considering objectives, limitations, multiplicity of analyses, results from similar studies, and other relevant evidence	15-18	
Generalisability	21	Discuss the generalisability (external validity) of the study results	15,16,18	
Other information				
Funding	22	Give the source of funding and the role of the funders for the present study and, if applicable, for the original study on which the present article is based	19,20	

*Give information separately for cases and controls in case-control studies and, if applicable, for exposed and unexposed groups in cohort and cross-sectional studies.

Note: An Explanation and Elaboration article discusses each checklist item and gives methodological background and published examples of transparent reporting. The STROBE checklist is best used in conjunction with this article (freely available on the Web sites of PLoS Medicine at <http://www.plosmedicine.org/>, Annals of Internal Medicine at <http://www.annals.org/>, and Epidemiology at <http://www.epidem.com/>). Information on the STROBE Initiative is available at www.strobe-statement.org.